J-OMINO PACKINGS

by

Janine E. Janoski

A thesis submitted to the Faculty of the University of Delaware in partial fulfillment of the requirements for the degree of Bachelor of Science in Mathematics with Distinction

Spring 2006

J-OMINO PACKINGS

by

Janine E. Janoski

Approved: _____

John A. Pelesko, Ph.D.
Professor in charge of thesis on behalf of the Advisory Committee

Approved: _____

Tobin A. Driscoll, Ph.D.
Committee member from the Department of Mathematics

Approved: _____

James L. Glancey, Ph.D.
Committee member from the Department of Bioresources Engineering

Approved: _____

Mohsen Badiey, Ph.D.
Chair of the University Committee on Student and Faculty Honors

ACKNOWLEDGEMENTS

I would like to acknowledge the advice and guidance of Dr. John A. Pelesko. Without Dr. Pelesko's dedication to academia this thesis would not have been possible. I also would like to thank Dr. Tobin A. Driscoll and Dr. James L. Glancey for being part of my thesis committee.

A special thanks to Dr. James Gleason and Lauren Rossi for the formulation of our early model. I finally would like to thank Dr. Richard Braun, Dr. Wenbo Li, Kara Lee Maki, and Kathryn Sharp, whom so graciously offered their time and support.

TABLE OF CONTENTS

LIST OF FIGURES

ABSTRACT

The question of how to efficiently pack objects has boggled the minds of some of the brightest mathematicians since the 17^{th} century. We will study the average number of empty spaces for a $1 \times j$ strip on a $1 \times n$ board. We are interested in comparing how different rules affect the average number of empty spaces seen on the $1 \times n$ board. We also wish to study and compare how different sizes, j, will affect the packing.

Next we focus on domino packings of the Aztec Diamond. It has been proven that a typical domino tiling of the Aztec Diamond contains an area where the dominoes are frozen into a brickwork pattern. This *frozen zone* shares a circular boundary with an inner disordered *temperate zone*. We are interested in comparing the structure for different rule sets for dominos on the Aztec Diamond. We will accomplish this task by using the Markov Chain Monte Carlo Method to study a typical packing for a given rule set on the Aztec Diamond.

Chapter 1

INTRODUCTION

The question of how to efficiently pack objects has boggled the minds of some of the brightest mathematicians since the 17^{th} century. Object packing appears in a wide variety of fields: coding theory, circuit design, bio-medical technology, industry, physics, and biology just to name a few. We will begin with a brief history of packings as well as a brief history of tilings.

1.1 History of Packings

The mathematical study of packings began in 1591 when Sir Walter Raleigh pondered the number of cannonballs that could fit in a stack. A close friend of Raleigh, Thomas Harriot who studied atomic theory, tried to convince Johannes Kepler to solve the problem [2]. Kepler's focus at this time was optics but today he is also known for studying planetary motion, regular polyhedra and logarithms [19]. When Harriot suggested that Kepler should merge atomic theory with his study of optics, Kepler was not interested. But then in 1611 Kepler published *De Nive Sexangula* which adopted an atomistic way to study the hexagonal shapes of snowflakes [2]. Kepler studied the shape of snowflakes by assuming their interiors were made of tiny spheres. He was interested in finding the most dense packing of these spheres. Thus we say that Kepler was interested in finding the void fraction for a three dimensional sphere packing.

Definition 1.1.1 Void Fraction- The void fraction of a packing is the ratio of the volume of empty spaces to the total volume. We denote the average void fraction as μ.

Kepler conjectured that the most dense sphere packing was 0.7404; i.e. the void fraction is 0.36.

Kepler did not prove this conjecture and in fact it was not proved for almost 400 years. Other famous mathematicians such as Johann Carl Friedrich Gauss studied packings. In the early $1800's$ Gauss demonstrated that the face-centered cubic structure is the densest crystalline three dimension packing [2]. At the start of the 20^{th} century new estimations of the original sphere packing bound that Kepler conjectured were proposed, yet there was still no proof. Several other mathematicians attempted to prove this conjecture yet none could accomplish this great feat. Finally Thomas Hale completed this difficult task in 1998, proving that Kepler's conjecture was correct.

Although the applications of three dimensional packings appear daily, two dimensional packings also serve as a great area of research and application. One of our biggest motivations for beginning research on packing was the two dimensional bio-disk device (Figure 1.1) used in the bio-medical field. The experimental set up for this model is as follows: A three dimensional plate contains five pathways with a square in the center connecting the pathways. One of these pathways serves as an inlet and the other four serve as outlets (Figure 1.2). The depth of the inlet and middle square is slightly larger then the diameter of beads which will be used for the experiment. The depth of the outlet pathways are slightly smaller then the diameter of the beads, so that the beads form a two dimensional packing in the inner square. A fluid mixed with the beads is forced through the inlet. We are interested in studying how the beads which remain in the inner square pack. It was found that if packed in such a manner then the inner square would be 94% completely packed

Figure 1.1: Here we see the bio-disk used in the bio-medical field [12].

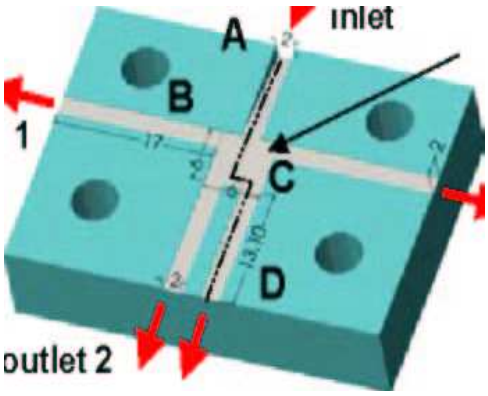

Figure 1.2: Experimental set up for the bio-disk device [12].

(Figure 1.3). It was also found that if we change the angle of the square to be 60 degrees 97% of the inner square would be completely packed (Figure 1.4).

This result leads us to ask how different boundaries affect a packing. Are there some shapes that naturally pack better then others? If this is the case are there any other examples of shapes which pack better then normal? It is clear that boundaries are not the only factor which affect how objects pack. It is obvious that the shape of the particle that we are packing will also have an affect on how efficiently a space S can be packed. We now turn our attention to one example of

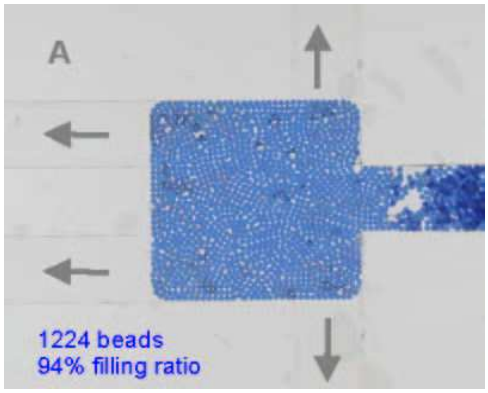

Figure 1.3: As the beads remain in the inner square chamber, we find a 94$ filling ratio [12].

particle shape, namely domino packings.

1.2 History of Domino Tilings and Packings

We begin with two definitions to differentiate a domino tiling and a domino packing.

Definition 1.2.1 Domino Tiling - A domino tiling of a given shape S consists of a collection of dominos which precisely cover S.

Definition 1.2.2 Domino Packing - A domino packing of a given shape S consists of a collection of dominos which either partially covers S or completely covers S.

One simple example of a domino packing is the *Tiling Classic* which leads us to Fibonacci's sequence. We define the Fibonacci sequence as follows:

Definition 1.2.3 Fibonacci Sequence- A Fibonacci Sequence is a sequence of integers, where each term in the sequence is the sum of the two previous terms. We denote the sequence where $F_0 = 1, F_1 = 1$ by $F_1, F_2, F_3, ...$ and find each term by $F_n = F_{n+1} + F_{n+2}$.

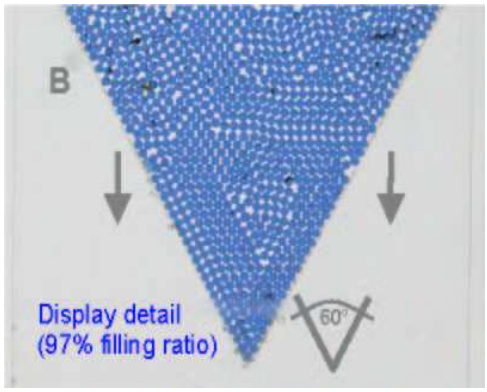

Figure 1.4: As we change the aperture angle to 60 degree, we find a 97% filling ratio[12].

The Tiling Classic is as follows:

> Using only 1×1 squares and 1×2 dominos one can pack a 1×3 strip of squares three different ways. In how many different ways can one pack a 1x15 strip of squares using only square tiles and dominos? [28]

We can begin to solve this problem by counting the simplest cases. For example, it is clear that if we have a 1×1 strip of squares there is only one way to tile it (namely by placing a 1x1 square on this strip). Similarly if we were to have a 1×2 strip there are two ways to tile it, either by one domino or two 1×1 squares. As stated in the problem there are three ways to tile a 1×3 strip. Thus we observe that the first three terms of are sequence are $1, 2, 3$, which is equivalently F_1, F_2, F_3. We notice that we can begin each packing with exactly one of two moves. Either we place a 1×2 domino or we place a 1×1 square. Hence the tiling for a $1 \times n$ strip can be determined from the tilings of a $1 \times (n-1)$ strip and a $1 \times (n-2)$ strip. Thus we see that we can tile a $1 \times n$ strip by exactly the the Fibonacci sequence, i.e. $F_n = F_{n+1} + F_{n+2}$.

We find that most one dimensional problems deal with packings rather than tilings (it would be quite boring to simply tile a strip using one shape). On the other hand there are several interesting two dimensional tiling problems. For example:

Given a checkerboard with a pair of diagonally opposite corner squares deleted is a domino tiling possible (Figure 1.5)?

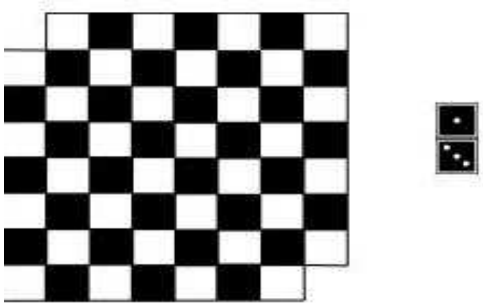

Figure 1.5: An 8x8 chessboard such that the Northwest and Southeast corners have been removed [20].

The answer is no, and its proof is remarkably simple. We see that the two corners we removed are of the same color, say black. We notice that each domino covers exactly two squares, one white and one black. Thus n dominos will cover n white squares and n black squares. But since in our chessboard there are more white squares then there are black such a tiling would be impossible [10].

There are several other similar problems which can come from different styles of chessboards using different polyominoes. One thing is certain from all these problems, the way a chessboard can be tiled depends on the shape of the board and the shape of the object. This makes way for more recent tiling explorations such as those of James Propp.

In the $1990's$ James Propp from the University of Wisconsin became interested in tiling research. While visiting MIT in the late $1990's$ Propp started an undergraduate research group that focused on tiling. Their most spectacular findings were those that they uncovered while studying the Aztec diamond.

Definition 1.2.4 Aztec Diamond- An Aztec Diamond of order n consists of all lattice point coordinates that lie inside $|x| + |y| \leq n + 1$ (Figure 1.6).

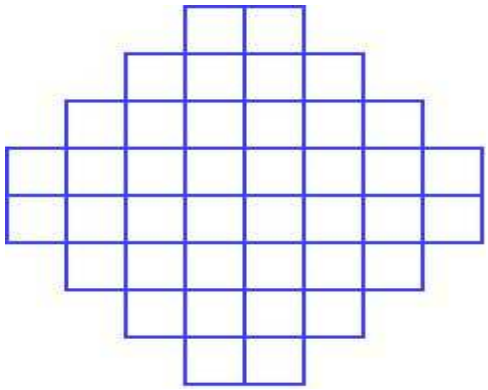

Figure 1.6: The Aztec Diamond consists of all coordinates that lie inside $|x|+|y| \leq n + 1$ [22].

Propp's research group was curious to see what would happen in an average Aztec Diamond domino tiling. Using the Markov Chain Monte Carlo Method to sample all possible tilings, Propp found that a completely tiled Aztec diamond has a very unique structure. It appeared that in each of the corners the dominos all faced the same direction and in the center the dominos created a temperate zone (Figure 1.7). Propp refereed to this notion as the Arctic Circle Phenomenon.

Definition 1.2.5 Arctic Circle Phenomenon - One can prove for a large Aztec Diamond, the polar regions (where the dominoes are *frozen* into a brickwork pattern) are almost always just the regions outside the inscribed circle [22].

Now we have seen how one particular object will pack a few simple spaces. Next we wish to study how different particles pack a given space. We conducted experiments using chains of different lengths to study how the packing changes as a function of chain length.

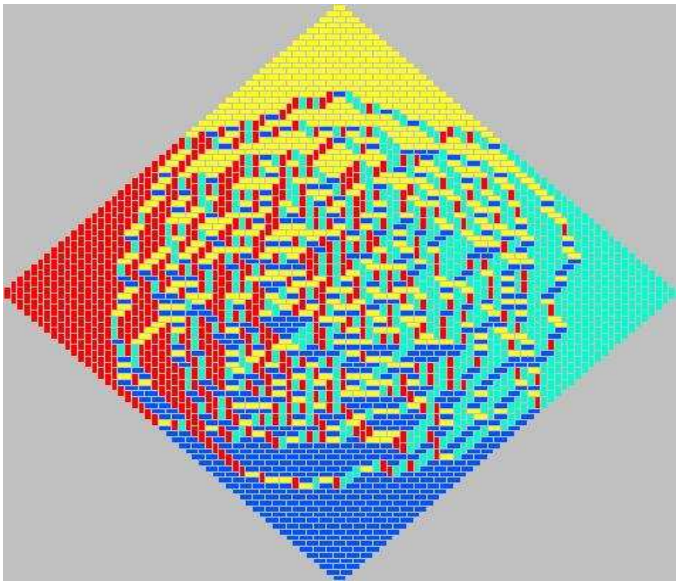

Figure 1.7: A typical tiling of the Aztec Diamond displays the Arctic Circle phenomenon [22].

1.3 Experimental Example of a Packing Model

In 2003 Stokely et. al. [27] began to study the two dimensional packing of granular materials. They were interested in studying the average packing fraction in particles with large aspect ratios as well as determining how the particle orientation would effect the packing. For their experiment they used acrylic rods of diameter $D = 0.16cm$ and length $L = 1.9cm$ (hence an aspect ratio of $\frac{D}{L} \simeq 12$. They placed the rods horizontally on a sheet of plexiglass and then secured a second piece of plexiglass on top of the first with a particle spacer $1.25cm$ in diameter. This allows the rods to move without overlapping [27]. We will use this experimental procedure as the basis for the design of our experiment.

We will focus our experimental work on the effects of particle shape on random and semi-random packing. To study the particle shape, we will be using chains to explore how a given chain length will effect the random packing.

1.3.1 A simple model

We begin our experiments with a simple model of a two dimensional chamber filled with polypropylene balls. In this portion of the experiment we wish to study the way that individual balls pack.

1.3.1.1 Set Up

Our basic setup and procedure is as follows; We create two dimensional packings by distributing 1/8 inch white polypropylene balls into a 12×12 inch chamber made from lexan. Two $12x12$ sheets of lexan were cut and held together by 7 screws (three along the left side, three along the right, and three along the bottom). Next we create an angle of 180 degrees to serve as a boundary along the bottom of the chamber . The boundary is made from lexan sheets with a height of 1/8 inch.

We also build a trough to filter in the balls. The top of the trough is a triangle shape, with an opening in the bottom slightly larger then 1/8 inch so the balls are able to be filtered into the chamber. There is an apparatus that stabilizes the trough so it can sit along the top of our chamber. The trough comes equipped with a stopper along the bottom that can be removed to start the flow of the balls. Figure 1.8 shows the set up.

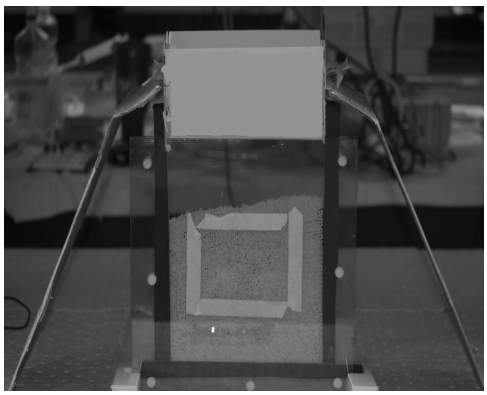

Figure 1.8: The experimental set up for our ball chamber

1.3.1.2 Experiment

We begin by filtering balls into the chamber through the trough. Behind the chamber we placed a black background and shine a light directly onto the chamber from above the camera. After taking a picture for each trial, we imported the pictures into Matlab. Once in Matlab we find the void space of the picture using the command

$$[iw, jw] = find(a(:, :, 1) > 128); \tag{1.1}$$

followed by

$$length(iw)/prod((size(a(:, :, 1)))). \tag{1.2}$$

The result produced from the second command calculates the void space for that particular picture. We repeat this process 10 times.

Note: We have found that with this procedure our computed void is within 1% of the actual void space. We found this percent error by running tests on the simple pictures. First we took a picture of just one ball and found the error when read into Matlab (This allowed us to check if it were reading the entire ball as white or if some error was taking place). Next we checked to see how Matlab read the black background (This checked to make sure Matlab read the black background as black, not with some error). Finally we took a picture containing a small number of balls (1,5,10,20) and had Matlab compute the void space of the picture compared with our own calculations of the void space in the picture by hand. We find that these calculations combined leave us with an error of less then 1%

After taking ten pictures we found the average void fraction to be 90.64%. Now that we have some starting point with a simple experiment we wish to modify our set up so that we can study how chains will pack in our two dimensional chamber.

1.3.2 Chains

1.3.2.1 Set Up

Our experimental set up for the Chain experiment will create a two dimension field in which the void fraction can be studied using chains. The chains are 3/16 inch enamel coated stainless steel chains. The chains were cut into lengths ranging from a length of 2 balls per chain to a length of 16 balls per chain. A chamber was made from two 12×12 inch plexiglass sheets. A boundary of 3/16 inch was created around the edges of the plexiglass (allowing the chains enough room to move without overlapping). A black sheet was attached to one of the two sheets of plexiglass serving as a background. The sheets of plexiglass were connected to a shaker. Following the procedure in the simple experiment we place a camera in front of the chamber and place a light above the camera.

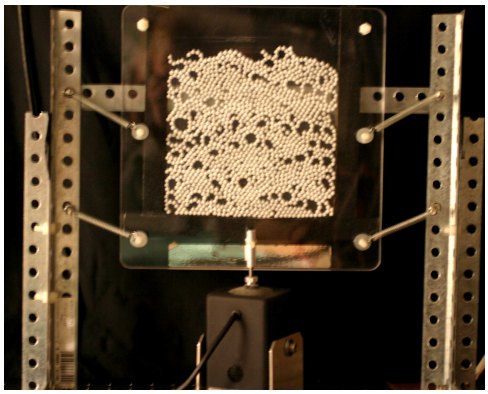

Figure 1.9: The set up for the chain set-up.

1.3.2.2 Experiment

Chains all of the same length were placed at random on one of the sheets of plexiglass. After the chains were placed, the second piece of plexiglass was secured on the first. The chamber was then turned vertical, allowing the chains to fall to the bottom of the chamber at random. We then shook the chamber for six minutes.

Shaking the chamber minimized the variation in the distribution of the void fraction for each chain length. We found that after six minutes of shaking there was no longer a change in variation. We then took a picture and uploaded it into Matlab, where a program counted the number of white pixels for a particular picture. The void fraction in turn was

$$1 - \frac{\text{number of white pixels}}{\text{total number of pixels}}. \tag{1.3}$$

We took 10 pictures from each chain length, and found the mean and standard deviation for each.

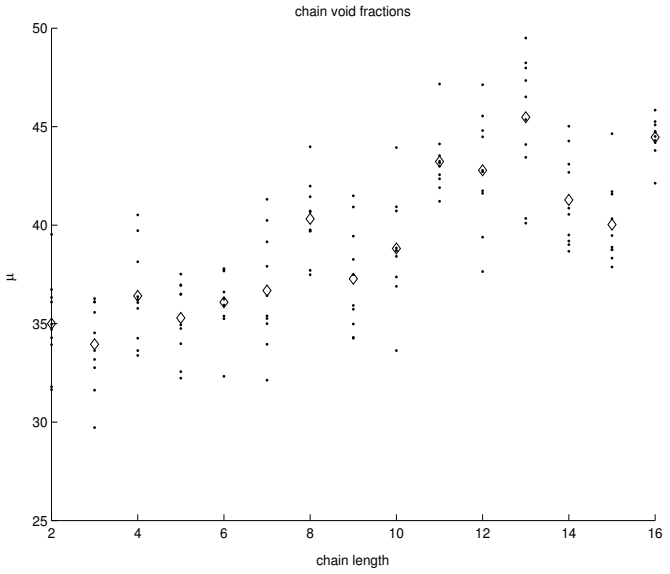

Figure 1.10: Plot of one of the 10 trials for each chain length (2 to 16).

Figure 1.10 shows the void fraction for each trial as well as the average void fraction. We see from our experiments that the void fraction is increasing as the length of the chain increases. Figure 1.11 shows a sample trial for each of the different length chains.

1.4 Remarks

The results of our experiment still need further analysis. We would be interested in identifying a specific trend which we see when we compare the void fraction to the size of the chain. We are also interested in following [27] to compare the aspect ratio to the size of our voids for each of the different lengths of the chains.

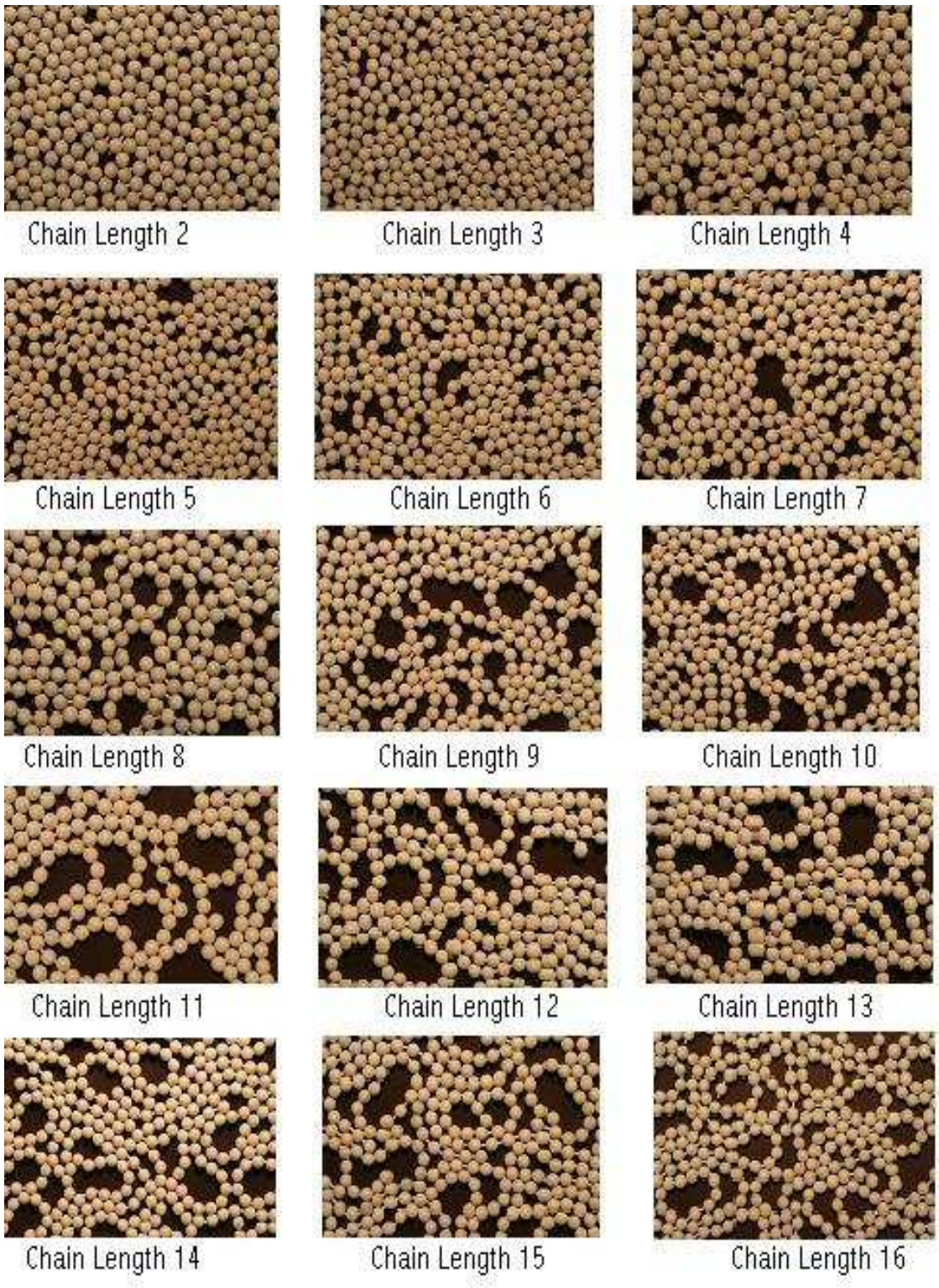

Figure 1.11: Plot of each of the 10 trials for each chain length (2 to 16).

Chapter 2

1-D MODELS

In the preceding chapter we have shown that the study of packings appear in many fields and have several applications. It is also apparent that the properties of the packings are affected by both particle shape and boundary conditions. Due to the varying types of packings, most research done in the area of packings is specialized with certain particles on a specified space. For our research we will focus on the behavior of one dimensional j-omino packings and domino packings on the Aztec Diamond.

2.1 Tight Packings

We consider a tight packing on a $1 \times n$ chessboard.

Definition 2.1.1 Tight Packing- A tight packing of a $1 \times n$ chessboard is a covering by $(1 \times j)$-ominoes and $1 \times (j-1)$ strips such that no two $1 \times (j-1)$ strips share an edge.

Our goal is to compute

$$\mu(n) = \text{Average Void Fraction} \tag{2.1}$$

where

$$\text{Void Fraction} = \frac{\text{Number of empty squares in a packing}}{n}. \tag{2.2}$$

We define two functions that let us count

$$c(n) = \#\text{ of ways to pack an } n \times 1 \text{ chessboard} \tag{2.3}$$

and

$$c(n,k) = \#\text{ of packings with exactly } k\text{-empty squares.} \tag{2.4}$$

We note that the number of voids in a packing can be written as

$$\sum_{k=0}^{n} kc(n,k), \tag{2.5}$$

and the void fraction can be written as

$$\sum_{k=0}^{n} \frac{k}{n} c(n,k). \tag{2.6}$$

Hence average void fraction is given by

$$\mu(n) = \frac{\sum_{k=0}^{n} \frac{k}{n} c(n,k)}{c(n)}, \tag{2.7}$$

We now wish to compute the average void fraction for several different tight j-omino cases. We begin with the tight domino case.

2.1.1 Dominos

We observe that $c(n)$ (and $c(n,k)$) are determined by the tiling of the first square on the chessboard as seen in Figure 2.1. Hence we can easily write a recursion for $c(n)$:

$$c(n) = c(n-3) + c(n-2). \tag{2.8}$$

The initial conditions satisfied by this recursion are $c(0) = c(1) = c(2) = 1$. We can construct a generating function (GF) for 2.8,

$$f(x) = \sum_{n=0}^{\infty} c(n)x^n. \tag{2.9}$$

Definition 2.1.2 Generating Function- A generating function is a power series $f(x) = \sum_{n=0}^{\infty} a_n x^n$ whose coefficients give the sequence $a_0, a_1, ...$ We will denote generating function as GF.

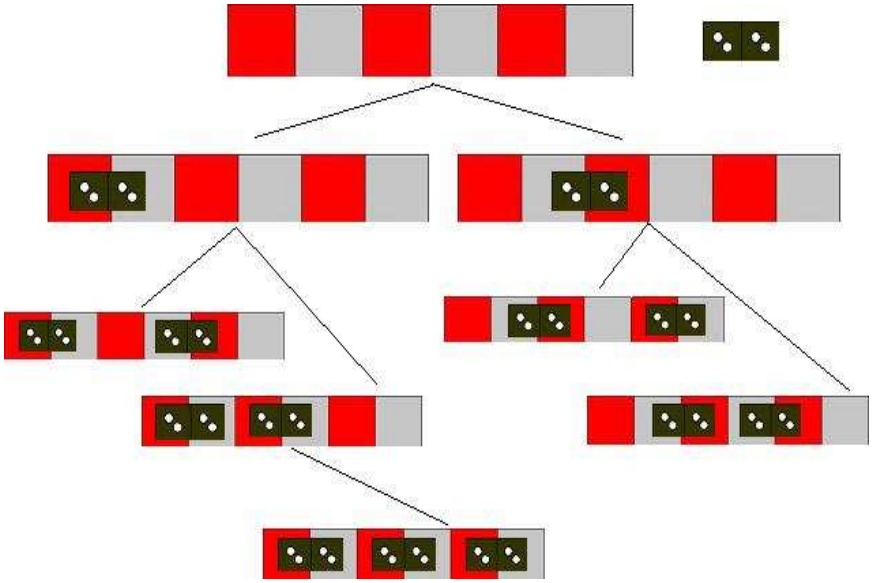

Figure 2.1: All possible tight packings for a 1x6 chessboard using 1x2 dominos.

Using our initial conditions, we can rewrite Equation 2.9 as

$$f(x) = 1 + x + x^2 + \sum_{n=3}^{\infty} c(n)x^n.$$

We multiply the recursion for $c(n)$ by x^n and sum from $n = 3$ to ∞ to find

$$\sum_{n=3}^{\infty} c(n)x^n = \sum_{n=3}^{\infty} (c(n-3) + c(n-2))x^n.$$

Thus we find

$$f(x) = \frac{1+x}{1-x^2-x^3}. \tag{2.10}$$

Next, we wish to consider this as a function of a complex variable,

$$f(z) = \frac{1+z}{1-z^2-z^3}. \tag{2.11}$$

It's easy to see that $f(z)$ has three singularities. One lies on the real axis, and two in the left half-plane, as seen in Figure 2.2. Numerically we find they are located at

$$z_0 \approx 0.755 \tag{2.12}$$

$$z_1 \approx -0.877 + 0.745i \tag{2.13}$$

$$\bar{z}_1 \approx -0.877 - 0.745i \tag{2.14}$$

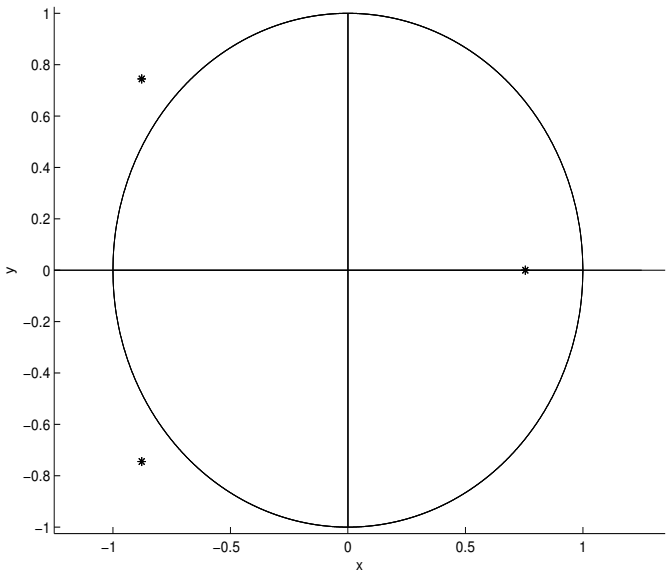

Figure 2.2: Plot of the three singularities of the generating function of a domino.

We also note

$$|z_0| \approx 0.755 \tag{2.15}$$

$$|z_1| = |\bar{z}_1| \approx 1.151 \tag{2.16}$$

We see that z_0 is the singularity closest to the origin. Computing the residue, a_{-1} of $f(z)$ at z_0 we find

$$a_{-1} = -\frac{1 + z_0}{2z_0 + 3z_0^2} \approx -0.545116. \tag{2.17}$$

Then we consider the function $g(z)$ obtained by subtracting this first singularity from $f(z)$, i.e.,

$$g(z) = \frac{1 + z}{1 - z^2 - z^3} - \frac{a_{-1}}{z - z_0} \tag{2.18}$$

Clearly $g(z)$ is analytic in a disk about the origin of radius $|z| < |z_1|$. Recall $|z_1| > 1$. This implies that the coefficients of the Taylor series expansion of $g(z)$, say

$$g(z) = \sum_{n=0}^{\infty} b_n z^n \tag{2.19}$$

satisfy

$$|b_n| \leq (\frac{1}{|z_1|} + \epsilon)^n \tag{2.20}$$

for all $\epsilon > 0$ as $n \longrightarrow \infty$ by Taylor's Theorem. Observe that

$$\frac{a_{-1}}{z - z_0} = -\sum_{n=0}^{\infty} \frac{a_{-1}}{z_0^{n+1}} z^n \tag{2.21}$$

and hence we have an asymptotic estimate for the $c(n)$

$$c(n) = -\frac{a_{-1}}{z_0^{n+1}} + O((\frac{1}{|z_1|} + \epsilon)^n) \tag{2.22}$$

as $n \longrightarrow \infty$ for all $\epsilon > 0$. More conveniently

$$c(n) \sim \frac{1 + z_0}{z_0^{n+1}(2z_0 + 3z_0^2)} \tag{2.23}$$

as $n \longrightarrow \infty$, where z_0 is the real root of $1 - z^2 - z^3 = 0$. We see that this is good approximation as early as $n = 10$. From the recursion we have $c(10) = 12$ and from the approximation we find $c(10) \approx 12.0184$.

We can proceed in a similar manner for $c(n, k)$. Our recursion is

$$c(n, k) = c(n - 2, k) + c(n - 3, k - 1) \tag{2.24}$$

with initial conditions

$$c(0, 0) = c(1, 1) = 1. \tag{2.25}$$

This recursion is then valid for *all* lattice points except the two where the initial conditions are defined. We define a GF for Equation 2.24,

$$h_n(x) = \sum_k c(n, k) x^k \tag{2.26}$$

where the sum is over all k and n is held fixed, but not equal to 0 or 1. Proceeding in the usual way we have

$$h_n(x) = h_{n-2}(x) + xh_{n-3}(x) \tag{2.27}$$

where $h_0(x) = 1$ and $h_1(x) = x$. Notice that

$$h_n'(1) = \sum_k kc(n,k) \tag{2.28}$$

and hence we compute $\mu(n)$ via

$$\mu(n) = \frac{h_n'(1)}{nc(n)}. \tag{2.29}$$

Thus if we solve for $h_n(x)$ we can solve $h_n'(1)$ and thus could solve for $\mu(n)$. We begin by building another GF. Let

$$g(y,x) = \sum_{n=0}^{\infty} h_n(x)y^n \tag{2.30}$$

and proceed as usual to find

$$g(y,x) = \frac{1+xy}{1-y^2-xy^3}. \tag{2.31}$$

We can again make estimates by investigating singularities. If $\alpha(x)$ is the real root of $1 - y^2 - xy^3$ we have

$$h_n(x) = \frac{1+\alpha(x)}{\alpha(x)^{n+1}(2\alpha(x)+3\alpha^2(x))} + O((\frac{1}{|\beta(x)|}+\epsilon)^n) \tag{2.32}$$

as $n \longrightarrow \infty$ for all $\epsilon > 0$. Now computing $h_n'(1)$ we find

$$\mu(n) = \frac{z_0}{2+3z_0} + \frac{2z_0}{n(2+3z_0)}. \tag{2.33}$$

As n tends to infinity we find

$$\mu(n) \sim \frac{z_0}{2+3z_0} \approx 0.177. \tag{2.34}$$

Figure 2.3 shows the accuracy of our $\mu(n)$ by comparing $\mu(n)$ such that $3 \leq n \leq 200$ against the exact value for $\mu(n)$. The exact value for $\mu(n)$ was computed by a computer program using the definition for average void fraction.

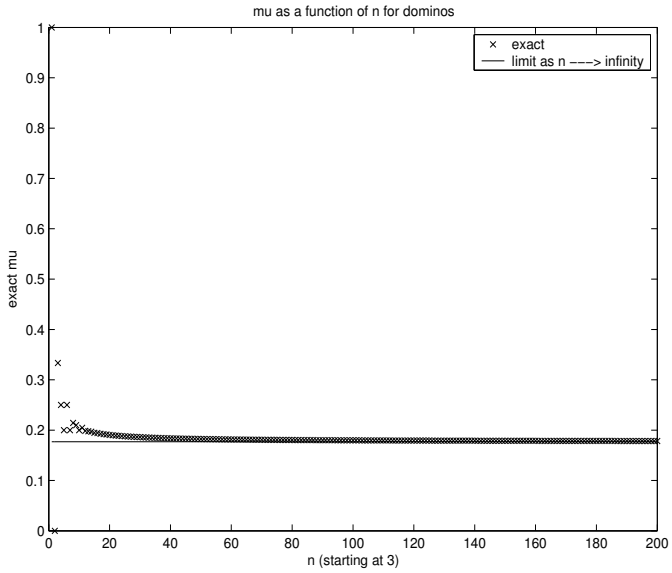

Figure 2.3: Plot of $\mu(n)$ as n goes from 3 to 200 vs. the limit as $n \longrightarrow \infty$

2.1.2 Tromino

Next we will compute the average void fraction for the 1×3 tromino case in the same manner as above. Thus we note that $c(n)$ (and $c(n,k)$) are determined by the tiling of the first two squares on the chessboard. Hence we can easily write a recursion for $c(n)$:

$$c(n) = c(n-3) + c(n-4) + c(n-5). \tag{2.35}$$

The initial conditions satisfied by this recursion are $c(0) = c(1) = c(2) = c(3) = 1$. Proceeding in the usual way we construct a GF

$$f(x) = \sum_{n=0}^{\infty} c(n)x^n. \tag{2.36}$$

Multiply the recursion for $c(n)$ by x^n and sum from $n = 4$ to infinity to find

$$f(x) = \frac{1 + x + x^2}{1 - x^3 - x^4 - x^5}. \tag{2.37}$$

Now, consider this as a function of a complex variable, i.e.

$$f(z) = \frac{1 + z + z^2}{1 - z^3 - z^4 - z^5}. \tag{2.38}$$

It's easy to see that $f(z)$ has five singularities. One of these singularities lies on the real axis, two lie on the unit circle and two in the left half-plane, which we can see in Figure 2.4 Numerically we find $z_0, z_2, \bar{z}_2$ and analytically we find $z_1, \bar{z}_1$ to be

$$z_0 \approx 0.755 \tag{2.39}$$

$$z_1 = i \tag{2.40}$$

$$\bar{z}_1 = -i \tag{2.41}$$

$$z_2 \approx -0.877 + 0.745i \tag{2.42}$$

$$\bar{z}_2 \approx -0.877 - 0.745i \tag{2.43}$$

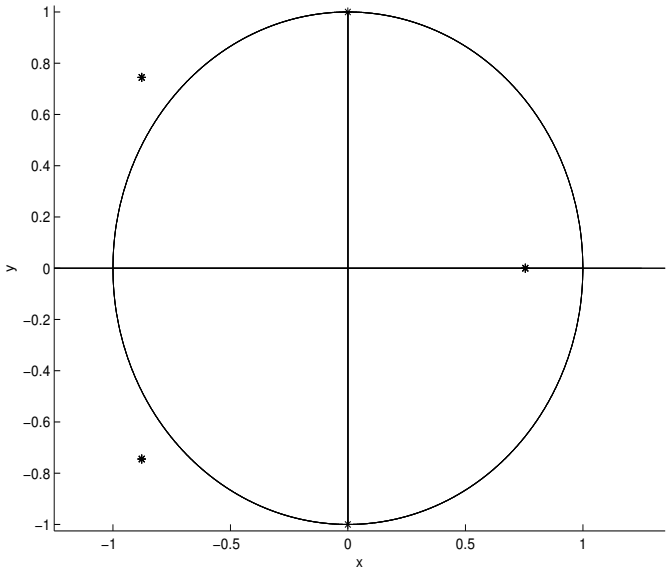

Figure 2.4: Plot of the five singularities of the generating function of a tromino

We also note

$$|z_0| \approx 0.755 \tag{2.44}$$

$$|z_1| = |\bar{z}_1| = 1 \tag{2.45}$$

$$|z_2| = |\bar{z}_2| \approx 1.151 \tag{2.46}$$

We see that z_0 is the singularity closest to the origin and z_1 and $\bar{z}_1$ lie on the unit circle. Computing the residue of $f(z)$ at z_0 we find

$$a_{-1}(z_0) = \frac{1 + z_0 + z_0^2}{-3z_0^2 - 4z_0^3 - 5z_0^4}. \tag{2.47}$$

Next we compute the residue of $f(z)$ at z_1 to find

$$a_{-1}(i) = \frac{i}{4i - 2}. \tag{2.48}$$

Finally we compute the residue of $f(z)$ at $\bar{z}_1$ to find

$$a_{-1}(-i) = \frac{-i}{-4i - 2} = \overline{a_{-1}(i)}. \tag{2.49}$$

Now we consider the function $g(z)$ obtained by subtracting the first three singularities

$$g(z) = \frac{1 + z + z^2}{1 - z^3 - z^4 - z^5} - \frac{a_{-1}(z_0)}{z - z_0} - \frac{a_{-1}(i)}{z - i} - \frac{a_{-1}(-i)}{z + i}. \tag{2.50}$$

Clearly $g(z)$ is analytic in a disk about the origin of radius $|z| < |z_2|$. Recall $|z_2| > 1$. This implies that the coefficients of the Taylor series expansion of $g(z)$, say

$$g(z) = \sum_{n=0}^{\infty} b_n z^n \tag{2.51}$$

satisfies

$$|b_n| \leq (\frac{1}{|z_2|} + \epsilon)^n \tag{2.52}$$

for all $\epsilon > 0$ as $n \longrightarrow \infty$. Now notice the following holds for $|z| < |z_0|$

$$\frac{a_{-1}(z_0)}{z - z_0} = -\sum_{n=0}^{\infty} \frac{a_{-1}(z_0)}{z_0^{n+1}} z^n, \tag{2.53}$$

$$\frac{a_{-1}(z_1)}{z - z_1} = -\sum_{n=0}^{\infty} \frac{a_{-1}(z_1)}{z_1^{n+1}} z^n, \tag{2.54}$$

$$\frac{a_{-1}(\bar{z}_1)}{z-\bar{z}_1} = -\sum_{n=0}^{\infty} \frac{a_{-1}(\bar{z}_1)}{\bar{z}_1^{n+1}} z^n \tag{2.55}$$

and hence we have an asymptotic estimate for the $c(n)$

$$c(n) = \frac{-a_{-1}(z_0)}{z_0^{n+1}} + \frac{-a_{-1}(z_1)}{z_1^{n+1}} + \frac{-a_{-1}(\bar{z}_1)}{\bar{z}_1^{n+1}} + O((\frac{1}{|z_2|}+\epsilon)^n) \tag{2.56}$$

as $n \longrightarrow \infty$ for all $\epsilon > 0$. More conveniently

$$c(n) \approx \frac{1+z_0+z_0^2}{z_0^{n+1}(3z_0^2+4z_0^3+5z_0^4)} + \frac{i}{i^{n+1}(-4i+2)} + \frac{i}{i^{n+1}(-4i-2)} \tag{2.57}$$

as $n \longrightarrow \infty$, where z_0 is the real root of $1-z^3-z^4-z^5=0$. We observe this is a good approximation as early as $n=10$. We have $c(10)=10$, from the approximation we find $c(10) \approx 10.12$. We can proceed in a similar manner for $c(n,k)$. Our recursion is

$$c(n,k) = c(n-3,k) + c(n-4,k-1) + c(n-5,k-2) \tag{2.58}$$

with initial conditions

$$c(0,0) = c(1,1) = c(2,2) = 1. \tag{2.59}$$

We define a GF for Equation 2.58

$$h_n(x) = \sum_k c(n,k)x^k \tag{2.60}$$

where the sum is over all k and n is held fixed, but not equal to 0, 1, or 2. Proceeding in the usual way we have

$$h_n(x) = h_{n-3}(x) + xh_{n-4}(4) + x^2 h_{h-5}(x) \tag{2.61}$$

where $h_0(x) = 1$, $h_1(x) = x$, and $h_2(x) = x^2$. Notice that

$$h_n'(1) = kc(n,k) \tag{2.62}$$

and hence we can compute $\mu(n)$ via

$$\mu(n) = \frac{h_n'(1)}{nc(n)} \tag{2.63}$$

We can build another GF

$$g(y,x) = \sum_{n=0}^{\infty} h_n(x) y^n \tag{2.64}$$

and find

$$g(y,x) = \frac{1 + xy + x^2y^2}{1 - y^3 - xy^4 - x^2y^5}. \tag{2.65}$$

Once again we can make estimates by investigating the singularities. If $\alpha(x)$ is the real root of $1 - y^3 - xy^4 - x^2y^5$ we have

$$h_n(x) = \frac{1 + x\alpha_0(x) + x^2\alpha_0^2(x)}{(3\alpha_0^2(x) + 4x\alpha_0^3(x) + 5x\alpha_0^4(x))\alpha_0^{n+1}} + O((\frac{1}{|\beta(x)|} + \epsilon)^n) \tag{2.66}$$

as $n \longrightarrow \infty$ for all $\epsilon > 0$. Now we can compute $\mu(n)$,

$$\mu(n) = \frac{z_0(1 + 2z_0)}{3 + 4z_0 + 5z_0^2} + \frac{(3z_0^3 + 36z_0^2 + 18z_0 + 6)z_0}{n(3 + 4z_0 + 5z_0^2)^2}. \tag{2.67}$$

As n tends to infinity we find

$$\mu(n) \sim \frac{z_0(1 + 2z_0)}{3 + 4z_0 + 5z_0^2} \approx 0.2136. \tag{2.68}$$

2.1.3 J-omino

Now that we have completed analysis of domino and tromino, we will now generalize to the j-omino case i.e. we are interesting in observing what happens as both $n \longrightarrow \infty$ and $j \longrightarrow \infty$. We generalize the recursion for $c(n)$ as

$$c(n) = \sum_{k=j}^{2j-1} c(n-k), \tag{2.69}$$

where $n > j$ and initial conditions are $c(n) = 1$ such that $0 \leq n \leq j$. Also we can determine a generalized form of the $c(n,k)$ recursion:

$$c(n,k) = \sum_{a=0}^{j-1} c(n-j-a, k-a) \tag{2.70}$$

Next we generalize the GF to find

$$f(x) = \frac{\sum_{a=0}^{j-1} x^a}{1 - \sum_{k=j}^{2j-1} x^k}. \tag{2.71}$$

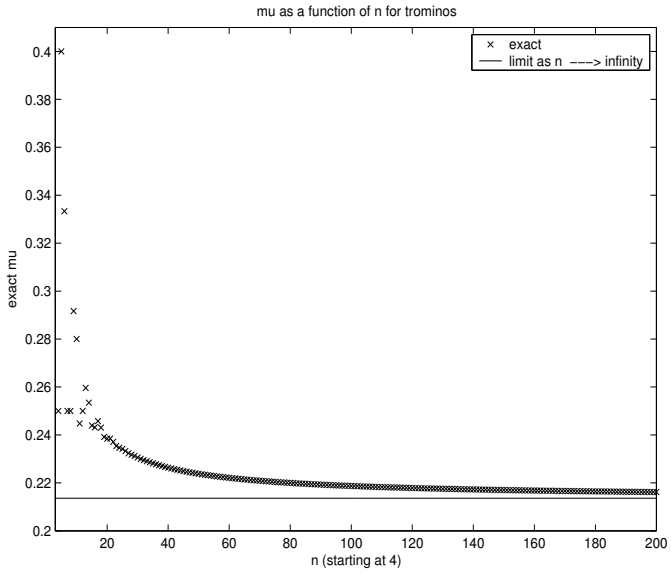

Figure 2.5: Plot of $\mu(n)$ for a tromino as n goes from 4 to 200 vs. the limit as $n \longrightarrow \infty$.

We are interested in considering $f(x)$ as a function of a complex variable $f(z)$. Again we wish to find the roots of $f(z)$. We notice that as our j-omino increases in size there are more roots inside the unit circle.

We examine Figure 2.6 and observe that both the trominos and 4-ominos have three singularities inside the unit circle. We also see that a 10-omino has 5 roots inside and a 15-omino has 8 roots inside. Finally we note that in Figure 2.7 has several singularities inside the unit circle. Visually it is clear that as j increases the number of singularities increase as well. Thus we are unable to generalize our theory as $j \longrightarrow \infty$, but we do obtain a procedure to compute the void fraction for a given j by following the analysis of the domino case.

2.1.4 Domino and Tromino Bucket

Next we wish to study what will happen in the case of a tight j-omino bucket.

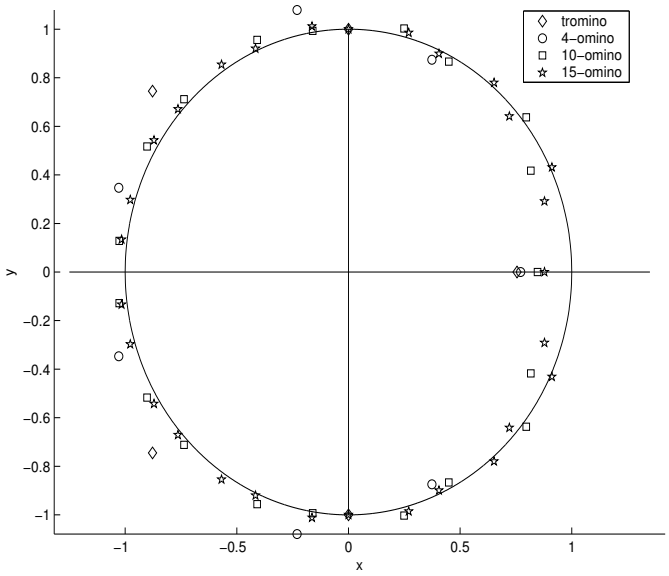

Figure 2.6: Plot of the singularities of the generating function for a domino, tromino, 4-omino, 10-omino, and 15-omino. We see that as j is increasing, the number of roots inside the unit circle is increasing.

Definition 2.1.3 Tight J-omino Bucket- A tight j-omino bucket of a $1 \times n$ chessboard is a covering by 1×2 dominos, 1×3 trominos, ... , $1 \times j$ j-ominos, 1×1 squares such that no two squares share an edge.

. We begin by analyzing a tight tromino bucket. Imagine we have a bucket of dominos and trominos. To create a tight packing of this type, we can choose a domino or tromino from the bucket and place it on the $n \times 1$ chessboard being careful to follow the same rules as before.

Since $c(n)$ is determined as usual by the tiling of the first square of the chessboard, we can write write a recursion for $c(n)$ as

$$c(n) = c(n-2) + 2c(n-3) + c(n-4) \tag{2.72}$$

(Figure 2.8 shows the ways to pack the first tile) where $c(n-3)$ is counted twice since we can start with a void followed by a domino or start with a tromino.

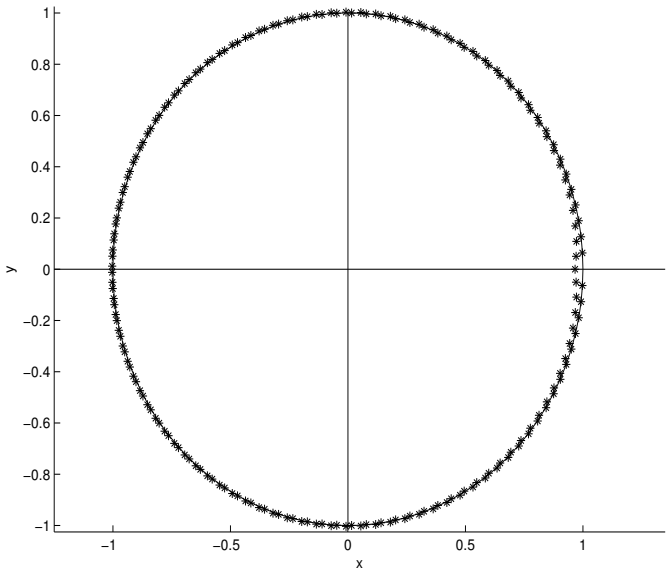

Figure 2.7: Plot of the singularities of the generating function of a 100-omino. We see here, that compared to Figure 2.6 there are more roots inside the unit circle.

The initial conditions of the recursion are $c(0) = c(1) = c(2) = 1$ and $c(3) = 3$. We can construct a GF given by

$$f(x) = \sum_{n=3}^{\infty} c(n)x^n. \tag{2.73}$$

Using our initial conditions we rewrite as

$$f(x) = 1 + x + x^2 + \sum_{n=0}^{\infty} c(n)x^n.$$

We can multiply the recursion for $c(n)$ by x^n and sum from $n = 3$ to ∞ to find

$$\sum_{n=3}^{\infty} c(n)x^n = \sum_{n=3}^{\infty} (c(n-2) + 2c(n-3) + c(n-4))x^n.$$

Calculating $f(x)$ in the usual way, we obtain

$$f(x) = \frac{1+x}{1 - x^2 - 2x^3 - x^4}. \tag{2.74}$$

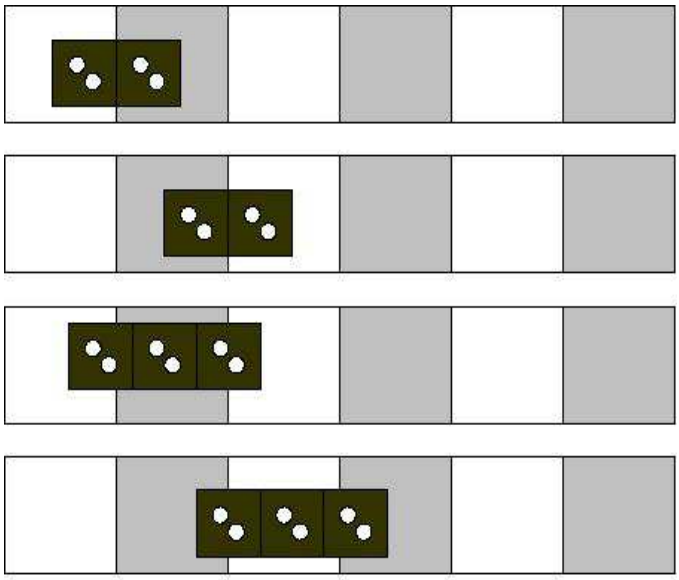

Figure 2.8: $c(n)$ is determined by tiling the first square of a chessboard. This figure shows us the choices we having for tiling the first space of a chessboard with dominos and trominos

Again we consider $f(x)$ as a function of a complex variable,

$$f(z) = \frac{1+z}{1-z^2-2z^3-z^4}. \tag{2.75}$$

We consider the singularities inside the $|z| < 1$, so we must find the roots of $1 - z^2 - 2z^3 - z^4$.

We solve exactly and find our four singularities are

$$z_0 = -\frac{1}{2} + \frac{\sqrt{5}}{2} \tag{2.76}$$

$$z_1 = -\frac{1}{2} - \frac{\sqrt{5}}{2} \tag{2.77}$$

$$z_2 = -\frac{1}{2} + \frac{1}{2}i\sqrt{3} \tag{2.78}$$

$$z_3 = -\frac{1}{2} - \frac{1}{2}i\sqrt{3} \tag{2.79}$$

It is also noteworthy that z_1 is the golden ratio and z_0 is the negative of the golden ratio. We next want to compute the residue of $f(z)$ at z_0 to find

$$a_{-1} = -\frac{1+z_0}{2z_0+6z_0^2+4z_0^3} \tag{2.80}$$

and consider $g(z)$ obtained by subtracting the singularity from $f(z)$ i.e.,

$$g(z) = \frac{1+z}{1-z^2-2z^3-z^4} - \frac{a_{-1}}{z-z_0}. \tag{2.81}$$

Using the same process as in the domino and tromino case and find

$$c(n) \approx \frac{1+z_0}{(2z_0+6z_0^2+4z_0^3)z_0^{n+1}} \tag{2.82}$$

We can proceed in a similar manner for $c(n,k)$. Our recursion is

$$c(n,k) = c(n-2,k) + c(n-3,k) + c(n-3,k-1) + c(n-4,k-1), \tag{2.83}$$

with initial conditions

$$c(0,0) = c(1,1) = 1. \tag{2.84}$$

We next define a GF for Equation 2.83

$$h_n(x) = \sum_k c(n,k)x^k \tag{2.85}$$

where the sum is over all k and n is held fixed but not equal to 0 or 1. Proceeding as before, we have

$$h_n(z) = h_{n-2}(z) + h_{n-3}(z) + z(h_{n-3} + h_{n-4}) \tag{2.86}$$

where $h_0(z) = 1$ and $h_1(z) = z$. As in the domino and tromino calculations we can compute $\mu(n)$ as

$$\mu(n) = \frac{h_n'(1)}{nc(n)}. \tag{2.87}$$

Next we build another GF,

$$g(y,x) = \sum_{n=0}^{\infty} h_n(x)y^n. \tag{2.88}$$

We find that

$$g(y,x) = \frac{1+xy}{1-y^2-y^3-xy^3-xy^4}. \tag{2.89}$$

We can again make estimates by investigating the singularities. If $\alpha(x)$ is the real root of $1-y^2-y^3-xy^3-xy^4$ we have

$$h_n(x) = \frac{1+x\alpha(x)}{(2\alpha(x)+3\alpha(x)^2+3x\alpha(x)^2+4x\alpha(x)^3)\alpha(x)^{n+1}+O((\frac{1}{|\beta(x)|}+\epsilon)^n)} \tag{2.90}$$

as $n \longrightarrow \infty$ for all $\epsilon > 0$. Next we can find $h_n'(1)$ and compute

$$\mu(n) = \frac{z_0}{2(2z_0+1)} + \frac{z_0(6z_0^2+6z_0+1)}{2(2z_0+1)(1+3z_0+2z_0^2)n}. \tag{2.91}$$

As n tends to infinity we have

$$\mu(n) \sim \frac{z_0}{2(2z_0+1)} \approx 0.1382. \tag{2.92}$$

2.1.5 J-omino Bucket

Next we can generalize the Bucket case. In the general case, the bucket will be filled with dominos, trominos, four-ominos,...,j-ominos. We are interested in finding the average void fraction as both $n \longrightarrow \infty$ and $j \longrightarrow \infty$. We can find a general formula for the recursion $c(n)$,

$$c(n) = c(n-2) + 2c(n-3) + ... + 2c(n-j) + c(n-(j+1)), \tag{2.93}$$

where $c(0) = c(1) = 1$ are our initial conditions and all $c(-n) = 0$. Proceeding as usual we next create a generating function for $c(n)$ and in general we find that

$$f(x) = \frac{1+x}{1-x^2-2x^3-...-2x^j-x^{j+1}}. \tag{2.94}$$

Next we must determine where the roots lie in relation to the unit circle. We will visually show that there is only one root inside the unit circle, and then we will prove it.

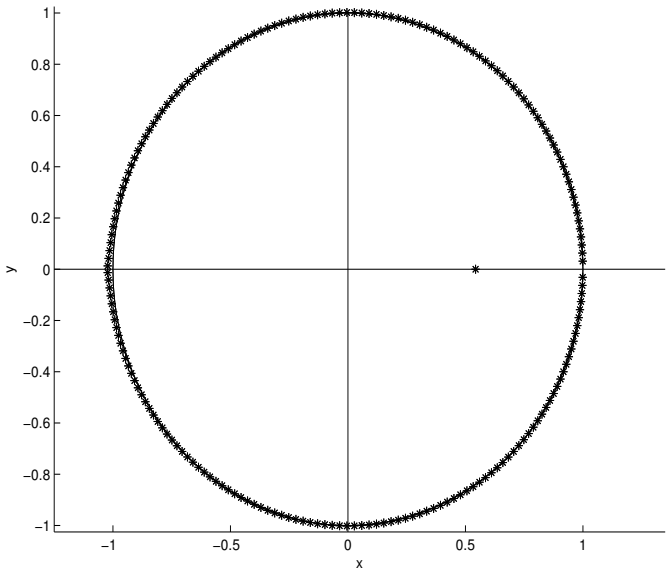

Figure 2.9: Plot of the roots of the generating function for bucket containing dominos up to 200-ominos.

Theorem 1. *There is only one root of* $f(z) = 1 - z^2 - 2z^3 - ... - 2z^j - z^{j+1}$ *inside the unit circle*

In order to prove Theorem 1 we will need to use Rouche's Theorem.

Rouche's Theorem: If f and h are each functions that are analytic inside and on a simple closed contour C and if the strict inequality

$$|h(z)| < |f(z)| \tag{2.95}$$

holds at each point on C then f and $f + h$ must have the same total number of zeros inside C.

Proof. We are interested in finding the roots of $f(z)$.

We can write $1 - z^2 - 2z^3 - ... - 2z^j - z^{j+1} = 1 - z^2 - z^{j+1} - 2z^2(1 + z + z^2 + ... + z^{j-2})$

$= 1 - z^2 - z^{j+1} - 2z^2\frac{1-z^j}{1-z}$ by geometric series.

Thus $1 - z - 3z^2 + z^3 = z^{j+2} - z^{j+1}$, which implies

$$1 - z - 3z^2 + z^3 + z^{j+1} - z^{j+2} = 0. \tag{2.96}$$

Hence we need only to investigate the number of roots of Equation 2.96.

Now we wish to use Rouche's Theorem to show that there is only one root inside the unit circle. We set $f(z) = 1 - z - 3z^2 + z^3$ and $h(z) = z^{j+2} - z^{j+1}$.

We rewrite z in polar form, i.e. $z = Re^{i\theta}$.

Thus $|f(z)| = |1 - z - 3z^2 + z^3| = |1 - Re^{i\theta} - 3Re^{i2\theta} + Re^{i3\theta}|$

$= |1 - R\cos(\theta) - iR\sin(\theta) - 3R\cos(2\theta) - i3R\sin(2\theta) + R\cos(3\theta) + iR\sin(3\theta)|$

$= \sqrt{(1 - R\cos(\theta) - 3R\cos(2\theta) + R\cos(3\theta))^2 + (R\sin(\theta) + 3R\sin(2\theta) + R\sin(3\theta))^2}$

$= \sqrt{1 + 11R^2 - 6R\cos(2\theta) + 2R\cos(3\theta) - 2R\cos(\theta) + \alpha}$,

where $\alpha = 6R^2(\cos(\theta)\cos(2\theta)+\sin(\theta)\sin(2\theta))-2R^2(\cos(\theta)\cos(3\theta)-\sin(\theta)\sin(3\theta))-6R^2(\cos(2\theta)\cos(3\theta) - \sin(2\theta)\sin(3\theta))$.

Now we minimize as a function of θ.

We see the minimum is at $\theta = \pi \longrightarrow |1 - z - 3z^2 - z^3|^2 = 9R^2 - 6R + 1$.

Computing $|f(z)|$ at $\theta = \pi$ we find,

$|f(z)| = \sqrt{1 - 6R + 9R^2} = \sqrt{(3R - 1)^2} = 3R - 1$.

Recall we wish to show $|h(z)| < |f(z)|$,

where $|h(z)| = |z^{j+2} - z^{j+1}| = |z^{j+1}(z - 1)| = |z^{j+1}||z - 1|$

$= |(Re^{i\theta})^{j+1}||Re^{i\theta} - 1|$

$= |R^{j+1}||(e^{i\theta})^{j+1}||R\cos(\theta) + iR\sin(\theta) + 1|$

$= |R^{j+1}||1^{j+1}|\sqrt{1 - 2R\cos(\theta) + R^2\cos^2(\theta) + R^2\sin^2(\theta)}$

$= |R^{j+1}|\sqrt{1 - 2R\cos(\theta) + R^2} = R^{j+1}\sqrt{1 - 2R\cos(\theta) + R^2}$.

Now we maximize as a function of θ. We find that the maximum is at $\theta = \pi \longrightarrow |z^{j+2} - z^{j+1}| = R^{j+1}(R + 1)$. Hence we wish to show $3R - 1 > R^{j+1}(R + 1) = R^{j+2} + R^{j+1}$.

Let $R = 1 - \epsilon$.

By substitution we wish to show $2-\epsilon > (1-\epsilon)^{j+2} + (1-\epsilon)^{j+1}$.

We can see from Figure 2.10 that if j is held fixed there exists an ϵ^* such that $f(z)$ has 1 root in the circle of radius $1-\epsilon$ for all $0 < \epsilon < \epsilon^*$

As we let $\epsilon \longrightarrow 0$ the theorem is proved. □

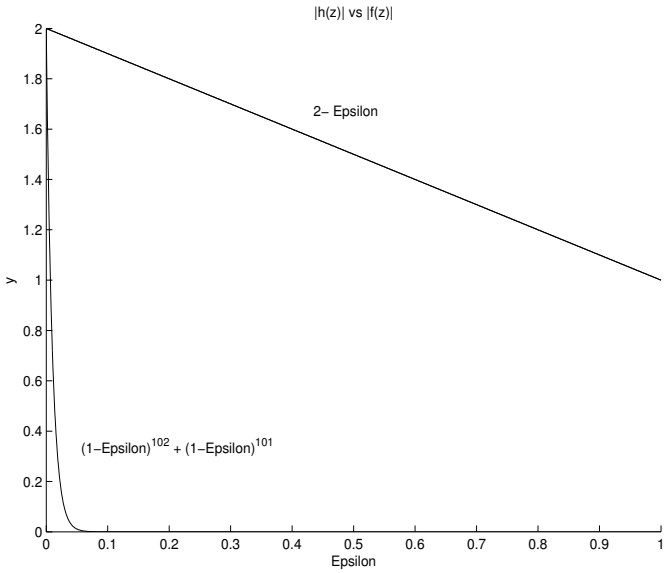

Figure 2.10: We see that for j fixed at 100, $|h(z)| < |f(z)|$ for ϵ sufficiently small.

We also notice that as $j \longrightarrow \infty$, $z_0 \longrightarrow 0.543689$. We can compute the residue for the general case at z_0 to be

$$a_{-1} = -\frac{1+z_0}{2z_0 + 6z_0^2 + ... + 2jz_0^{j-1} + (j+1)z_0^j}. \tag{2.97}$$

Here we can also find that our $g(z) = f(z) - \frac{a_{-1}}{z-z_0}$. Following the usual method, in general

$$c(n) \simeq \frac{1+z_0}{(2z_0 + 6z_0^2 + ... + 2jz_0^{j-1} + (j+1)z_0^j)z_0^{n+1}}. \tag{2.98}$$

We can also find a general formula for the $c(n,k)$,

$$c(n,k) = \sum_{a=2}^{j} c(n-a,k) + \sum_{b=3}^{j+1} c(n-b,k-1), \tag{2.99}$$

with initial conditions $c(0,0) = c(1,1) = 1$. Creating another GF, h_n, we find

$$h_n(x) = \sum_{a=2}^{j} h_{n-a}(x) + x \sum_{b=3}^{j+1} h_{n-b}(x). \tag{2.100}$$

Creating another generating function $g(y,x)$ we find that

$$g(y,x) = \frac{1+xy}{1 - \sum_{a=2}^{j} y^a - x\sum_{b=3}^{j+1} y^b}. \tag{2.101}$$

If we say $\alpha(x)$ is the real root of $1 - \sum_{a=2}^{j} y^a - x\sum_{b=3}^{j+1} y^b$ we have

$$h_n(x) = \frac{1+x\alpha(x)}{j(x)} + O((\frac{1}{|\beta(x)|} + \epsilon)^n), \tag{2.102}$$

where

$$j(x) = \alpha^{n+1}(\sum_{a=1}^{j-1}(a+1)\alpha^a(x) + \sum_{b=2}^{j} x(b+1)\alpha^b(x)) \tag{2.103}$$

as $n \longrightarrow \infty$ for all $\epsilon > 0$. Using Equation 2.29, we find

$$\mu(n) \simeq \frac{\sum_{b=3}^{j+1} z_0^6}{z_0(2z_0 + 2(3z_0^2 + ... + jz_0^{j-1}) + (j+1)z_0^j)}. \tag{2.104}$$

As n tends to infinity we find

$$\mu(n) \approx 0.099388. \tag{2.105}$$

2.2 Non-Tight Packings

We define a non-tight packing as follows,

Definition 2.2.1 Non-Tight Packing- A Non-Tight Packing of a $1 \times n$ chessboard is a covering by $1 \times j$ j-ominoes and 1×1 squares with no restrictions.

Once again we are interested in finding the average void fraction for several cases.

2.2.1 Domino

We again begin by explore non-tight packings of the domino case. It is clear that $c(n)$ (and $c(n,k)$) are determined by the tiling of the first square. We can write a recursion for $c(n)$:

$$c(n) = c(n-1) + c(n-2). \tag{2.106}$$

The initial conditions satisfied by this recursion are $c(0) = c(1) = 1$ and $c(2) = 2$. Proceeding in the usual way we find

$$f(z) = \frac{1}{1 - z - z^2}. \tag{2.107}$$

We find the two singularities for $f(z)$ are

$$z_0 = 0.618 \tag{2.108}$$

$$z_1 = -1.118. \tag{2.109}$$

We compute the residue for $f(z)$ at z_0 to find

$$a_{-1} = -\frac{1}{1 + 2z_0} \tag{2.110}$$

and consider

$$g(z) = \frac{1}{1 - z - z^2} - \frac{a_{-1}}{(z - z_0)}. \tag{2.111}$$

Using the same method as for tight packings we find

$$c(n) \approx \frac{1}{z_0^{n+1}(1 + 2z_0)}. \tag{2.112}$$

Proceeding in the usual way we find

$$c(n,k) = c(n-1,k-1) + c(n-2,k), \tag{2.113}$$

where $c(0,0) = c(1,1) = 1$. We define a generating function $h_n(x)$, where

$$h_n(x) = xh_{n-1}(x) + h_{n-2}(x). \tag{2.114}$$

We compute $g(y,x)$ to be

$$g(y,x) = \frac{1}{1-xy-y^2}. \tag{2.115}$$

If $\alpha(x)$ is the real root of $1-xy-y^2$ we have

$$h_n(x) = \frac{1}{(2\alpha(x)+x)\alpha(x)^{n+1}} + O((\frac{1}{|\beta(x)|}+\epsilon)^n). \tag{2.116}$$

Using 2.29, we find as n tends to infinity

$$\mu(n) \sim \frac{1}{1+2z_0} \approx 0.447. \tag{2.117}$$

2.2.2 Tromino

We can compute the average void fraction for a non-tight packing by 1×3 trominos. It is clear that

$$c(n) = c(n-1) + c(n-3), \tag{2.118}$$

where the initial conditions are satisfied by $c(0) = c(1) = c(2) = 1$ and $c(3) = 2$. Proceeding in the usual method we find

$$f(x) = \frac{1}{1-x-x^3}. \tag{2.119}$$

Considering this as a function of a complex variable we find the three singularities and see that

$$|z_0| \approx 0.6823 \tag{2.120}$$

$$|a_1| = |a_2| \approx 1.21. \tag{2.121}$$

We compute the residue at z_0 to find

$$a_{-1} = -\frac{1}{1+3z_0^2} \tag{2.122}$$

and consider

$$g(z) = \frac{1}{1-z-z^3} - \frac{a_{-1}z_0}{z-z_0}. \tag{2.123}$$

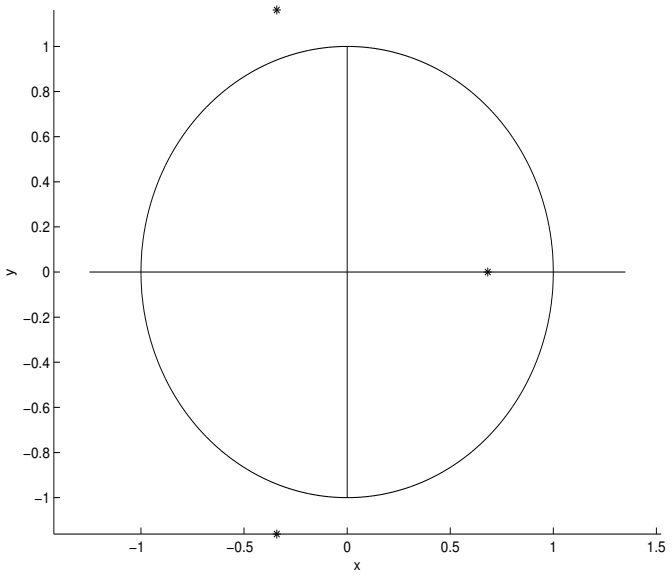

Figure 2.11: Plot of the singularities for a tromino.

Thus we find

$$c(n) \approx \frac{1}{(1+3z_0^2)z_0^{n+1}}. \tag{2.124}$$

Continuing as usual we find

$$c(n,k) = c(n-1,k-1) + c(n-3,k), \tag{2.125}$$

where $c(0,0) = c(1,1) = 1$. We create two generating functions $h_n(x)$ and $g(y,x)$ where,

$$h_n(x) = xh_{n-1}(x) + h_{n-3}(x) \tag{2.126}$$

and

$$g(y,x) = \frac{1}{1-xy-y^3}. \tag{2.127}$$

If $\alpha(x)$ is the real root of $1 - xy - y^3$ we have

$$h_n(x) = \frac{1}{(x+3\alpha(x)^2)\alpha(x)^{n+1}} + O((\frac{1}{|\beta(x)|}+\epsilon)^n). \tag{2.128}$$

Thus

$$\mu(n) \simeq \frac{1}{1+3z_0^2} \approx 0.4173 \tag{2.129}$$

2.2.3 J-omino

Now that we have completed analysis of non-tight packings of dominos and trominos, we will attempt generalize this analysis for $n \longrightarrow \infty$ and $j \longrightarrow \infty$. We generalize the recursion for $c(n)$ as

$$c(n) = c(n-1) + c(n-j), \tag{2.130}$$

where $n > j$ and initial conditions are $c(i) = 1$, for all $i < j$ and $c(j) = 2$. Also we can determine a generalized form of the $c(n,k)$ recursion:

$$c(n,k) = c(n-1,k-1) + c(n-j,k). \tag{2.131}$$

Next we generalize the GF to find

$$f(x) = \frac{1}{1-x-x^j}. \tag{2.132}$$

We are interested in considering $f(x)$ as a function of a complex variable $f(z)$. Again we wish to find the roots of $f(z)$. We notice that as our j-omino increases in size there are more roots inside the unit circle.

First we observe that in Figure 2.12 the behavior of the singularities that lie on $|z| < 1$ increase as j increases. For a tromino we have one singularity, a 6-omino has 3 singularities, a 12-omino has 5 singularities, and an 18-omino has 7 singularities. Finally in Figure 2.13 shows that for a 100-omino there are several singularities that lie inside the unit circle. In order to analytically determine our $\mu(n)$ we must subtract off the residues of any roots inside the unit circle. Since this number is increasing we cannot generalize our solution using the same methods as in the domino and tromino case.

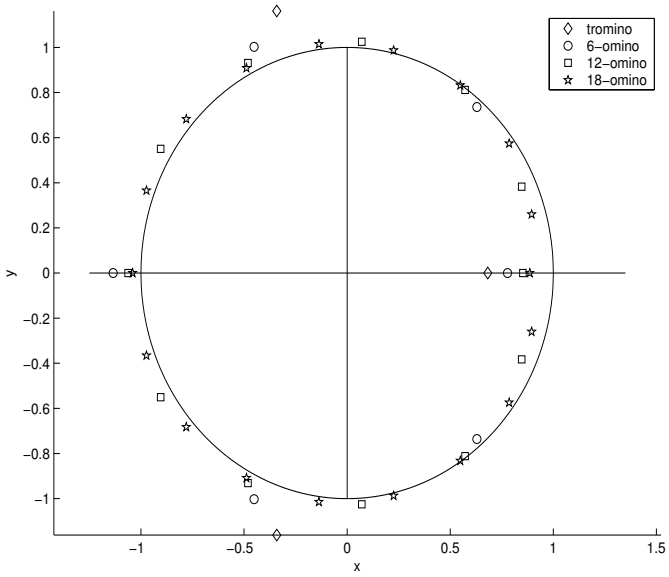

Figure 2.12: Plot of the singularities of the non-tight generating function for a tromino, 6-omino, 12-omino, and 18-omino. We see that as j is increasing, the number of roots inside the unit circle is increasing.

2.2.4 Domino and Tromino Bucket

We explore the idea of a bucket of dominos and trominos as we did for the tight case.

Definition 2.2.2 Non-tight j-omino bucket- A non-tight j-omino bucket of a $1 \times n$ chessboard is a covering by 1×2 dominos, 1×3 trominos, ... , $1 \times j$ j-ominos, and 1×1 squares with no restrictions.

It is clear that we can find a recursion for $c(n)$ based on the tiling of the first square, i.e.

$$c(n) = c(n-1) + c(n-2) + c(n-3), \tag{2.133}$$

where $c(0) = c(1) = 1, c(2) = 2$, and $c(3) = 4$. We create a GF, $f(x)$, and consider it as a function of complex variables,

$$f(z) = \frac{1}{1 - z - z^2 - z^3}. \tag{2.134}$$

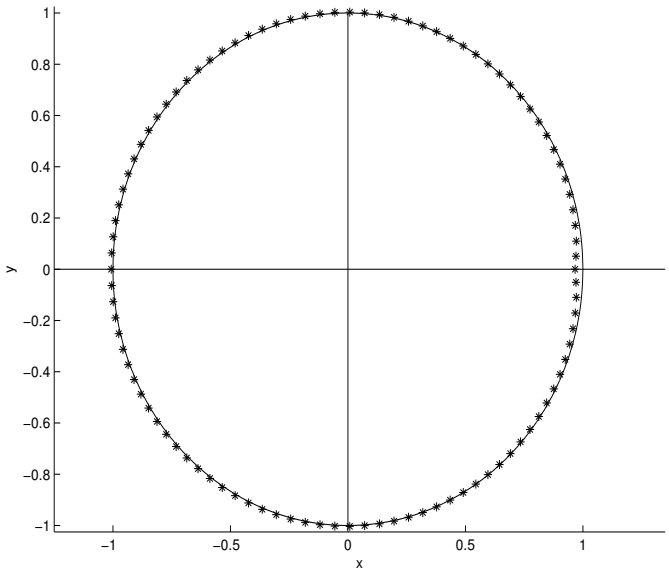

Figure 2.13: Plot of the singularities of the non-tight generating function of a 100-omino. We see here, that compared to Figure 2.12 the number of roots inside the unit cirlce has increased.

We find the three singularities,

$$|z_0| \approx 0.5437 \tag{2.135}$$

$$|z_1| = |z_2| \approx 1.356. \tag{2.136}$$

We compute the residue at z_0,

$$a_{-1} = -\frac{1}{1 + 2z_0 + 3z_0^2} \tag{2.137}$$

and find

$$c(n) \approx \frac{1}{(1 + 2z_0 + 3z_0^2)z_0^{n+1}}. \tag{2.138}$$

It is clear that

$$c(n, k) = c(n - 1, k - 1) + c(n - 2, k) + c(n - 3, k), \tag{2.139}$$

where $c(0, 0) = c(1, 1) = 1$. We create two GF $h_n(x)$ and $g(y, x)$, where

$$h_n(x) = xh_{n-1}(x) + h_{n-2}(x) + h_{n-3}(x) \tag{2.140}$$

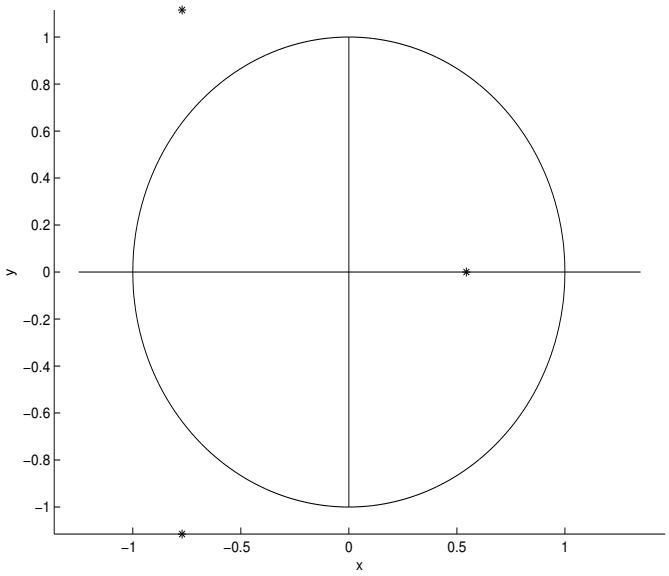

Figure 2.14: Plot of the singularities for a domino and tromino bucket.

and

$$g(y,x) = \frac{1}{1 - xy - y^2 - y^3}. \tag{2.141}$$

Proceeding in the usual way we find

$$\mu(n) = \frac{1}{1 + 2z_0 + 3z_0^2 + 4z_0^3} + \frac{2z_0 + 6z_0^2 + 12z_0^3}{(1 + 2z_0 + 3z_0^2 + 4z_0^3)^2 n} \tag{2.142}$$

As $n \longrightarrow \infty$

$$\mu(n) \simeq \frac{1}{1 + 2z_0 + 3z_0^2 + 4z_0^3} \approx 0.3636 \tag{2.143}$$

2.2.5 J-omino Bucket

Next we can generalize the Bucket case. In the general case, the bucket will be filled with dominos, trominos, 4-ominos,...,j-ominos. We can find a general formula for the recursion $c(n)$,

$$c(n) = c(n-1) + c(n-2) + ... + c(n-j), \tag{2.144}$$

where $c(0) = c(1) = 1$ are our initial conditions and all $c(-n) = 0$. Proceeding as usual we next create a generating function for $c(n)$ and in general we find that

$$f(x) = \frac{1}{1 - x - x^2 - ... - x^j}. \tag{2.145}$$

Next we must determine where the roots lie in relation to the unit circle. We visually see from Figure 2.15 that for a 200-omino bucket there is only one root inside the unit circle. Now we wish to prove that for any j there is only one root inside the unit circle.

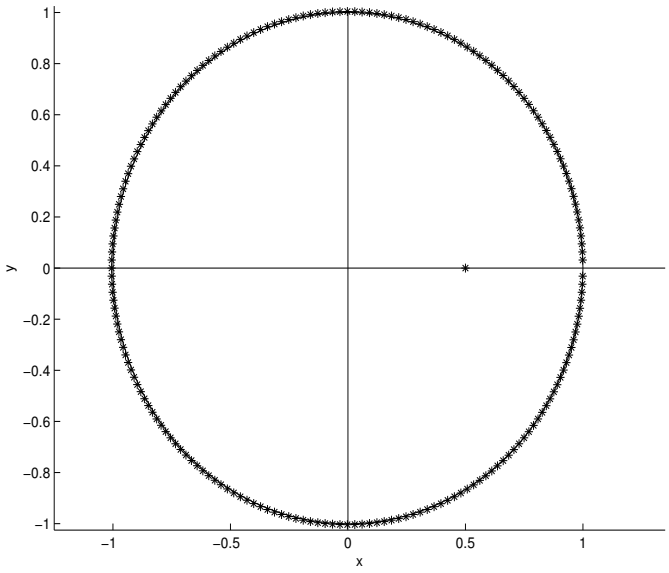

Figure 2.15: Plot of the singularities for a bucket up to 200-ominos.

Theorem 2. *There is only one root of* $f(z) = 1 - z - z^2 - ... - z^j$ *inside the unit circle*

In order to prove Theorem 2 we will need to use Roche's Theorem.

Rouche's Theorem: If f and h are each functions that are analytic inside and on a simple closed contour C and if the strict inequality

$$|h(z)| < |f(z)| \tag{2.146}$$

holds at each point on C then f and f+h must have the same total number of zeros inside C.

Proof. We are interested in finding the roots of $f(z)$.
We can write $1 - z - z^2 - ... - z^j = 1 - z(1 + z + z^2 + ... + z^{j-1}) = 1 - z\frac{1-z^j}{1-z}$ by geometric series.
Thus $1 - z = z - z^{j+1}$, which implies

$$1 - 2z + z^{j+1} = 0. \tag{2.147}$$

Hence we need only to investigate the number of roots of 2.147.
Now we wish to use Rouche's Theorem to show that there is only one root inside the unit circle. We set $f(z) = 1 - 2z$ and $h(z) = z^{j+1}$.
We rewrite z in polar form, i.e. $z = Re^{i\theta}$.
Thus $f(z) = |1 - 2z| = |1 - 2Re^{i\theta}| = |1 - 2R\cos(\theta) - i2R\sin(\theta)|$
$= \sqrt{(1 - 2R\cos(\theta))^2 + 4R^2\sin(\theta)^2} = \sqrt{1 - 4R\cos(\theta) + 4R^2(\cos(\theta)^2 + \sin(\theta)^2)}$,
which simplifies to $\sqrt{1 - 4\cos(\theta) + R^2}$.
Thus $|1 - 2z|^2 = 1 - 4R\cos(\theta) + 4R^2$.
Now we minimize as a function of θ.
We see the minimum is at $\theta = 0 \longrightarrow |1 - 2z|^2 = 1 - 4R + 4R^2$.
Computing $|f(z)|$ at $\theta = 0$ we find,
$|f(z)| = \sqrt{1 - 4R + 4R^2} = \sqrt{(2R - 1)^2} = 2R - 1$.
Recall we wish to show $|h(z)| < |f(z)|$,
where $|h(z)| = |z^{j+1}| = |(Re^{i\theta})^{j+1}| = |R^{j+1}||(e^{i\theta})^{j+1}| = |R^{j+1}||1^{j+1}| = |R^{j+1}| = R^{j+1}$.
Hence we wish to show $2R - 1 > R^{j+1}$.
Let $R = 1 - \epsilon$.
By substitution we wish to show $1 - 2\epsilon > (1 - \epsilon)^{j+1}$.

We can see from Figure 2.16 that if j is held fixed there exists an $\epsilon*$ such that $f(z)$ has 1 root in the circle of radius $1-\epsilon$ for all $0 < \epsilon < \epsilon*$
As we let $\epsilon \longrightarrow 0$ the theorem holds. □

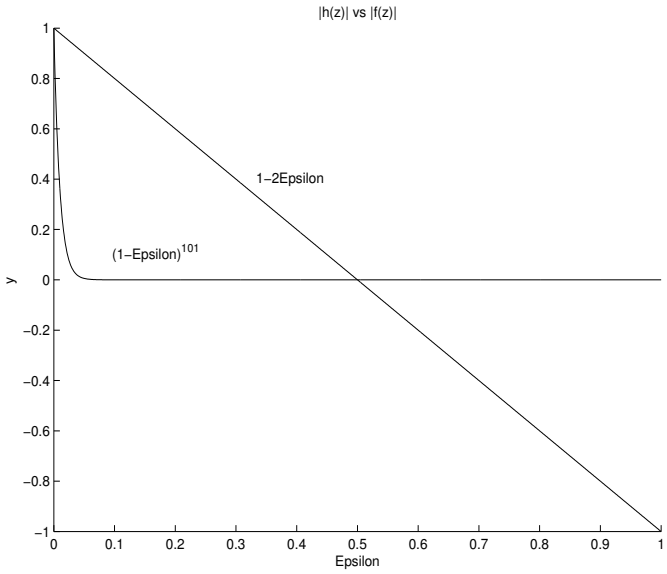

Figure 2.16: We see that for j fixed at 100, $|h(z)| < |f(z)|$ for ϵ sufficiently small.

We notice that as $j \longrightarrow \infty$, $z_0 \longrightarrow 0.5$. We compute the reside for the general case at z_0 to be

$$a_{-1} = -\frac{1}{1 + 2z_0 + 3z_0^2 + ... + jz_0^{j-1}}. \tag{2.148}$$

Here we can also find that our $g(z) = f(z) - \frac{a_{-1}}{z-z_0}$. Following the usual method, in general

$$c(n) \simeq \frac{1}{(1 + 2z_0 + 3z_0^2 + ... + jz_0^{j-1})z_0^{n+1}}. \tag{2.149}$$

We can also find a general formula for the $c(n,k)$,

$$c(n,k) = c(n-1,k-1) + \sum_{a=2}^{j} c(n-a,k), \tag{2.150}$$

with initial conditions $c(0,0) = c(1,1) = 1$. Creating another GF, h_n, we find

$$h_n(x) = xh_{n-1}(x) + \sum_{a=2}^{j} h_{n-a}(x). \tag{2.151}$$

Creating another generating function $g(y,x)$ we find that

$$g(y,x) = \frac{1}{1 - xy - \sum_{a=2}^{j} y^a}. \tag{2.152}$$

If we say $\alpha(x)$ is the real root of $1 - xy - \sum_{a=2}^{j} y^a$ we have

$$h_n(x) = \frac{-1}{j(x)} + O((\frac{1}{|\beta(x)|} + \epsilon)^n), \tag{2.153}$$

where

$$j(x) = \alpha^{n+1}(\sum_{a=1}^{j-1}(a)\alpha(x)^{a-1}) \tag{2.154}$$

as $n \longrightarrow \infty$ for all $\epsilon > 0$. Using Equation 2.29, we find

$$\mu(n) \simeq \frac{1}{1 + 2z_0 + 3z_0^2 + ... + jz_0^{j-1}}. \tag{2.155}$$

As n tends to infinity we find

$$\mu(n) \approx 0.25. \tag{2.156}$$

2.3 Concluding Remarks

We see that for any type of packing we can find the average void fraction by applying the processes laid out for the tight domino packing case. We see in Figure 2.17 the average void fraction for all the cases which we have computed. We also note that we cannot generalize our packing theory to a j-omino case due to the behavior of the roots of the complex function $f(z)$. For our bucket theory, we see that the roots of $f(z)$ behave nicely allowing us to generalize to a j-omino bucket.

Packing Type	μ(n)
Tight Domino	0.177
Tight Tromino	0.2136
Tight Tromino Bucket	0.1382
Tight Jomino Bucket	0.099388
Non-Tight Domino	0.447
Non-Tight Tromino	0.4173
Non-Tight Tromino Bucket	0.3636
Non-Tight Jomino Bucket	0.25

Figure 2.17: The average void fraction for each different type of packing. We note that for the tight j-omino bucket and non-tight j-omino bucket we find the average void fraction as $j \longrightarrow \infty$

Chapter 3

2-D MODELS

Our two dimensional models will be based on computer simulations of different types of packings of the Aztec diamond. Recall,

Definition 3.0.1 Aztec Diamond- An Aztec diamond of order n consists of all lattice point coordinates that lie inside $|x| + |y| \leq n + 1$ (Figure 1.6).

On this diamond we will explore domino tilings, j-omino tilings, tight packings, non-tight packings, and finally we will define a new packing, a restricted packing.

The findings of our work lies nested in Matlab simulations. We are interested in finding what the typical packing was for all the cases mentioned above. We will use order 18 Aztec Diamonds for our simulations. In order to find this typical packing we will use the Markov Chain Monte Carlo Method. Monte Carlo Methods are numerical methods that utilize sequences of random numbers to perform an approximate calculation. Markov Chains are collections of random variables X_t (where the index t runs through 1,2, ...) having the property that the current state, t, depends only on the previous state, $t - 1$. Markov Chain Monte Carlo Method samples from a given state space with a given probability distribution by constructing a Markov Chain that has the desired distribution as its stationary distribution.

Thus the method that we will use for the following simulations will be as following:

- We begin with a given set of rules which will allow us to step from one state to the next. These rules must allow us to reach all possible packings.
- We begin at any random packing and then take a random walk through the set of all possibly packings by applying this rule $500,000,000$ times.
- At the end of our random walk the distribution of our packing will be uniform. Thus we will see a *typical* packing [22].

Note that the trickiest part of the Markov Chain Monte Carlo method is knowing how many steps to take during the random walk in order to get the correct distribution. This is a very widely debated topic and there are several algorithms which attempt to solve the problem. Unfortunately we do not use these highly complicated algorithms for our simulations. We will express a little later why we believe that the number of steps we talk through our walk, 500,000,000, is sufficient. We now begin with the Domino Tiling as seen in [22]

3.1 Domino Tiling

As stated in Chapter 1 there has been a significant amount of research done on Domino Tilings on the Aztec Diamond. We will begin by explaining our algorithm found in aztecWalkDomTiling found in Appendix B. We will review the properties of tiling as well as show why we believe our methods are sufficient.

As stated above we need a rule in order to randomly walk through the set of all possible domino tilings on the aztec diamond. We will use the rule seen in [22], which we will refer to as the Rotation Rule. The Rotation Rule is as follows: Randomly choose a 2×2 square in the aztec diamond. We then check to see what is packing into this area.

Case 1: If we find that there are two dominos, we simply rotate the dominos. For example if we find two vertical dominos we rotate these dominos so that we have two horizontal dominos (Figure 3.1).

Case 2: If there is any other combination of dominos and pieces of dominos we do nothing.

Each time we apply this rule, we consider the move a step. We apply 500,000,000 steps to find our typical tiling. Figure 3.2 shows our domino tiled aztec diamond.

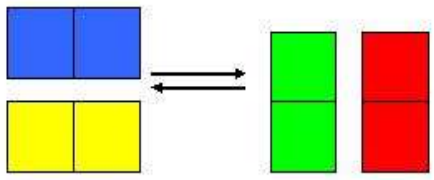

Figure 3.1: If we find two vertical dominos we replace them with two horizontal dominos and vise versa.

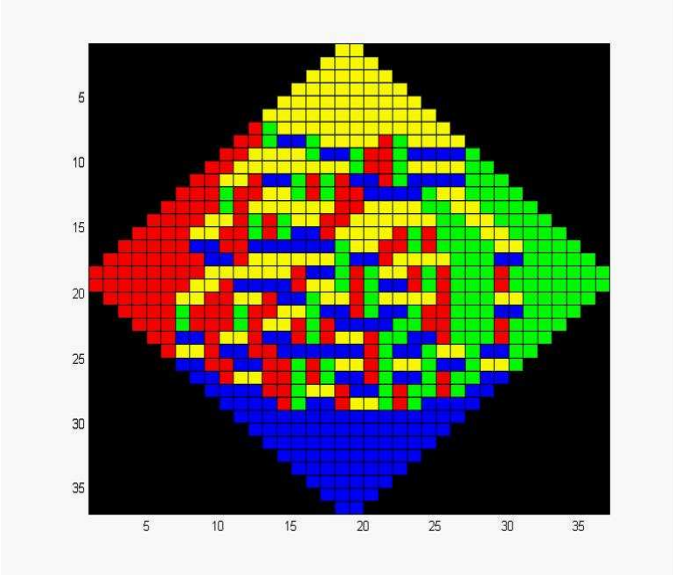

Figure 3.2: The aztec diamond tiled with dominos.

Figure 3.2 shows the Arctic Circle Phenomenon mentioned in [22]. By running this simulation a several times and seeing the desired result we believe that 500,000,000 steps in our walk would be sufficient to achieve the uniform distribution

we want from the Markov Chain Monte Carlo Method. Also we believe that an order 18 aztec diamond will be sufficient enough to see if any other types of packings have similar properties.

3.2 J-omino Tiling

Next we explore whether if other j-ominos display the Article Circle Phenomenon when they tile the Aztec Diamond.

Theorem 3. *The only j-omino that can tile an Aztec Diamond is the domino.*

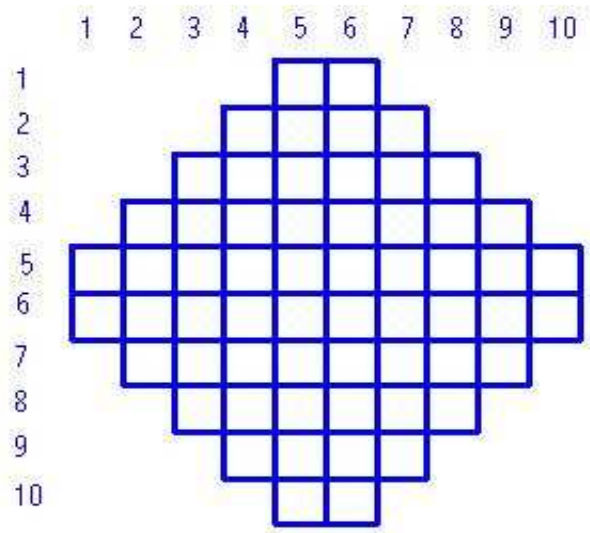

Figure 3.3: The Aztec Diamond.

Proof. (By way of contradiction)
Suppose we wish to tile an order n Aztec Diamond using a j-omino where $j > 2$.
Assume such a tiling exists.
We begin by examining what we can place in the top row of the diamond.
Since $j > 2$ we cannot place a j-omino horizontally.

Thus in the leftmost top square we will place a vertical j-omino.

Now left us move the the leftmost square in the second row.

Clearly since we placed a vertical j-omino in the leftmost square of the top row, the second column of the second row will contain a piece of that j-omino.

Thus we must place a vertical j-omino starting in the first column of the second row.

We notice that this pattern will continue until we reach the leftmost square in $\frac{order}{2}$ row of the Aztec Diamond.

It is clear that we cannot place a horizontal j-omino in the first column of the $\frac{order}{2}$ row.

Thus we must place a vertical j-omino.

But the first column of the $\frac{order}{2}$ contains only one square below it, the first column of the $\frac{order}{2} + 1$ row.

But $j > 2$.

Thus we cannot place a j-omino vertically.

Contradiction.

Hence the only j-omino that can tile the Aztec Diamond is the domino. □

3.3 Non-Tight Packings

Now that we have seen how a tiling behaves on the Aztec Diamond, we are interested in exploring what happens if we allow any number of empty spaces. In other words we will see how our non-tight packings, as defined in Chapter 2, behave on an order 18 Aztec Diamond.

Once again we begin by creating a rule that will allow us to walk the entire space of possible non-tight aztec packings. For this type of packing we wish to be able to add vertical dominos, remove vertical dominos, add horizontal dominos, and remove horizontal dominos. If we accomplish these four tasks then we will be able to create any possible packing. Thus the rule in this case is simple, we choose at random either a 1×2 or 2×1 rectangle from the Aztec Diamond and see what is

contained in that rectangle.

Case 1: If we find a domino, we remove it

Case 2: If we find two empty spaces, we place a domino

Case 3: If we are not in Case 1 or Case 2 we do nothing

Again we consider each application of this rule as a step and wish to complete 500,000,000 steps on our random walk. Running this simulation multiple times we find that our typical non-tight aztec diamond packing looks like Figure 3.4. It is evident from the Figure 3.4 that the Arctic Circle Phenomenon has disappeared.

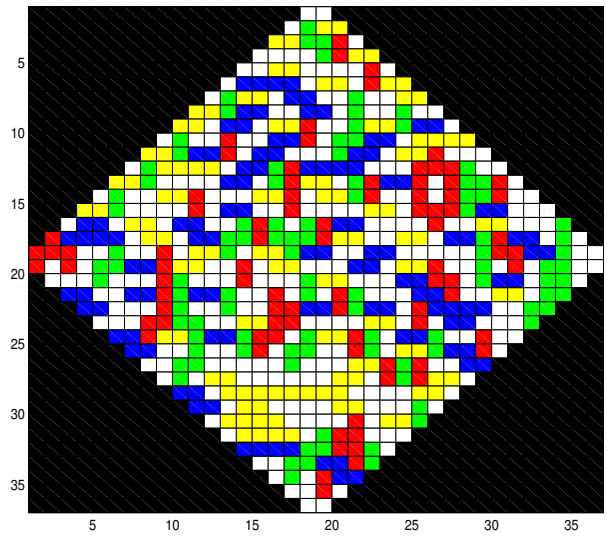

Figure 3.4: After 500,000,000 steps on an order 18 Aztec Diamond, we see that a non-tight Aztec Diamond has no order.

We are interested in examining how the number of empty spaces changes as we randomly walk throughout the set of all possible non-tight Aztec Diamond packings. Figure 3.5 shows the void fraction throughout our random walk. It appears that the typical non-tight random packing will contain between 30% and 40% voids.

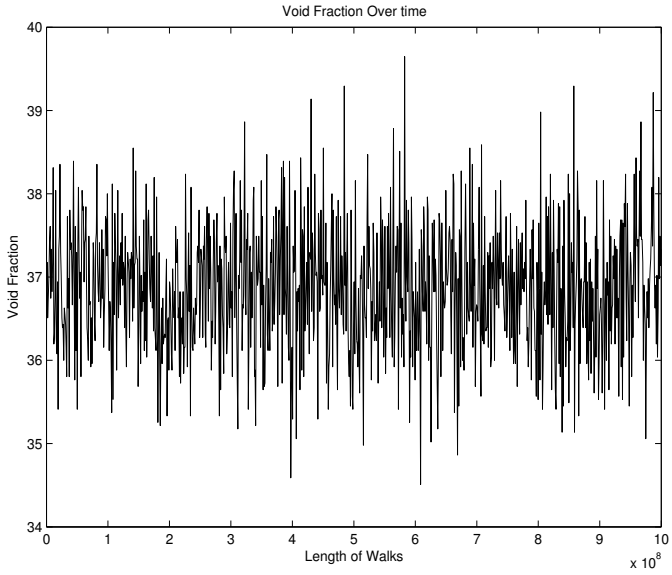

Figure 3.5: We see how the void fraction changes as the number of walks on the given packing increases.

3.4 Restricted Tilings

Now we know that the beautiful structure we saw in the domino tiling of the Aztec Diamond is not due to the shape of the Aztec Diamond alone. Clearly how we are packing the Aztec Diamond will affect the structure. So we next ask where exactly does the structure break down? How many empty spaces will cause the structure of the Aztec Diamond to vanish?

We define a new type of packing.

Definition 3.4.1 Restricted Tiling- A restricted tiling is a non-tight packing with a specified number of 1×1 empty spaces.

We are interested in how restricted domino tilings will change as the number of empty spaces increases.

For this new type of packing we need a more complicated rule to allow us to walk through the set of all possible restricted packings. We want to be able to move

the empty spaces anywhere in the Aztec Diamond and to change the orientation of the dominos. In this case we will define a step as applying the following two rules to the tiling.

1. The Rotation Rule
2. The Slide Rule (Figure 3.6)

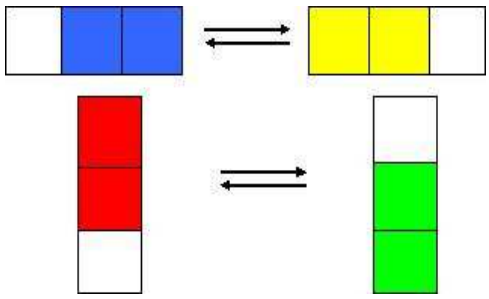

Figure 3.6: The Aztec Diamond tiled with dominos.

The slide rule is as follows: we begin by choosing at random one square inside the Aztec Diamond.

Case 1: We find that this random square is empty. We then check to see if there is a vertical domino above or below the square and a horizontal domino to the left or to the right of the square. For whichever of these cases apply, we at random choose a domino and slide it into the empty space. If there are no possible dominos to slide into the empty space we do nothing.

Case 2: We are not in Case 1, we do nothing.

We will take several walks on restricted tilings ranging from two void restricted tilings to fifty void restricted tilings (Figures 3.7 - 3.12). We see from the 2 void restricted tiling that the Arctic Circle Phenomenon is already beginning to deteriorate. Looking through the samples we see that as the number of voids increases the structure in the diamond collapses further. It is clear that by the time

we have 50 voids the Arctic Circle structure in the diamond is unrecognizable.

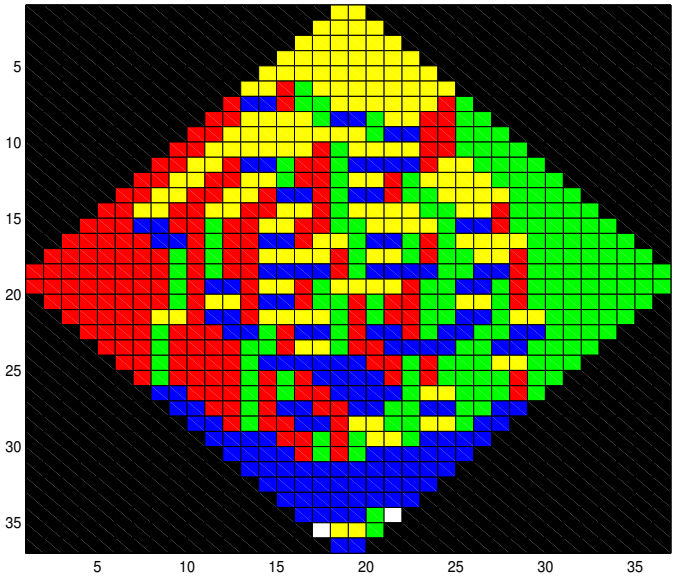

Figure 3.7: The Aztec Diamond with 2 voids after we apply the random walk five hundred million times.

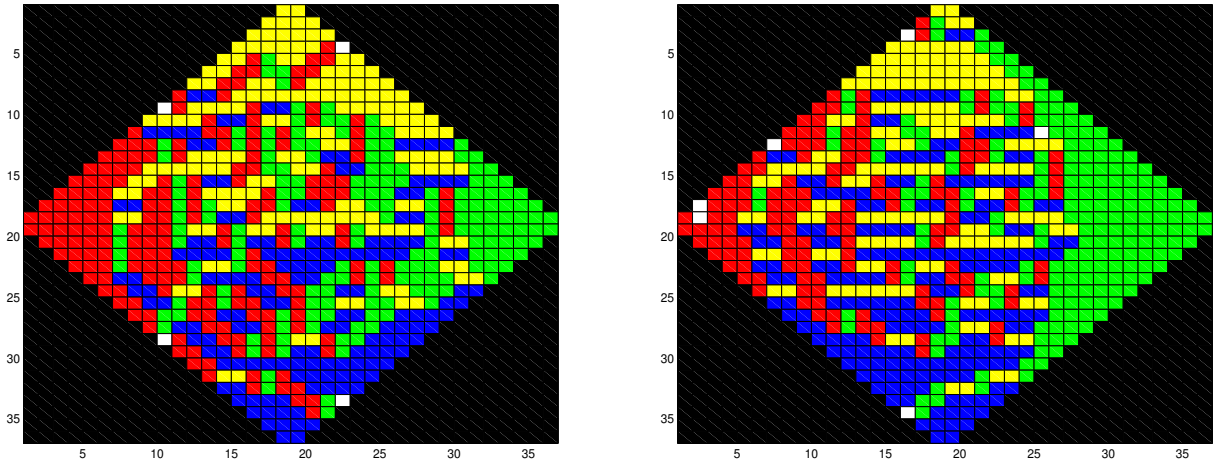

(Left) 4 Restricted (Right) 6 Restricted

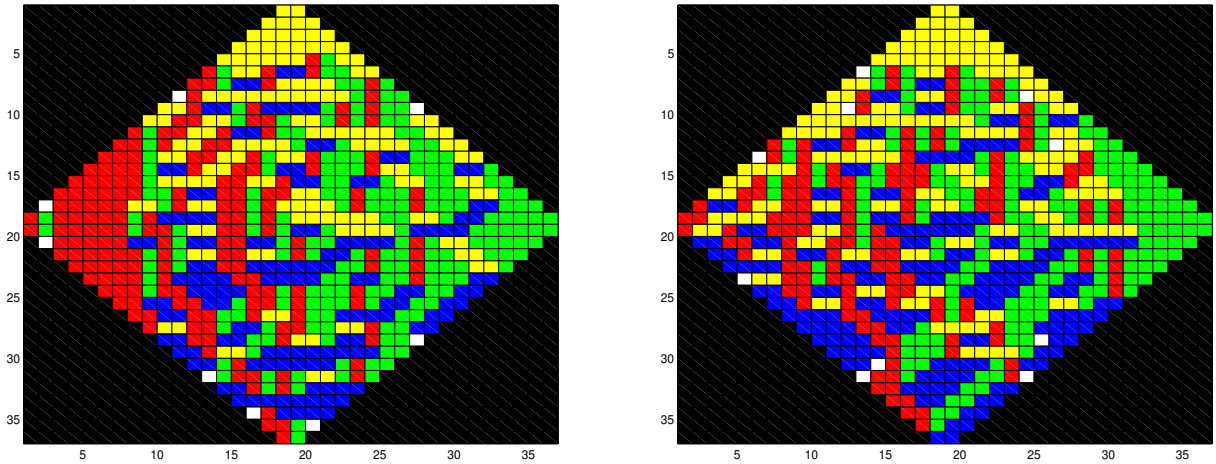

(Left) 8 Restricted (Right) 10 Restricted

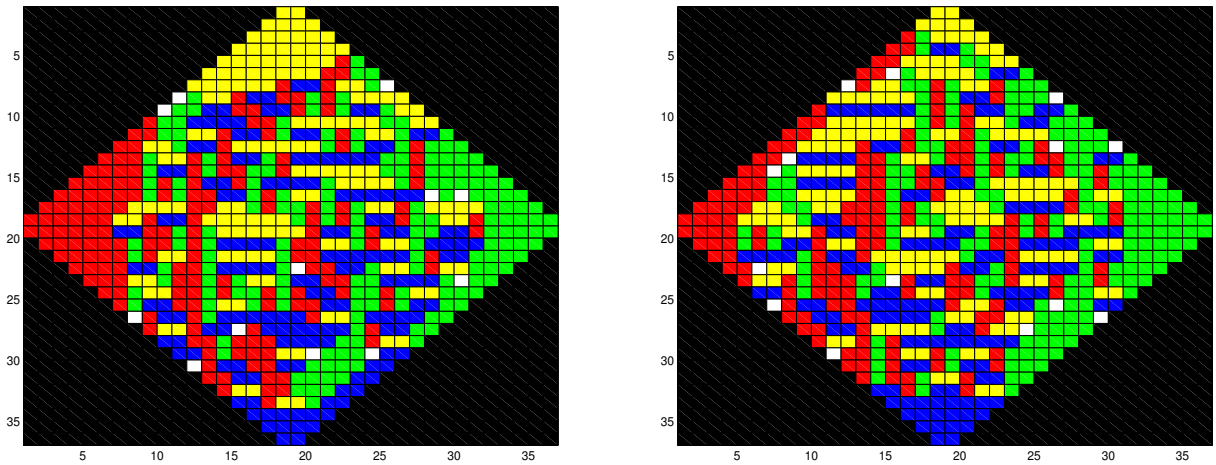

(Left) 12 Restricted (Right) 14 Restricted

Figure 3.8: We see a typical 4 Restricted Domino Aztec Diamond Tiling - a typical 14 Restricted Domino Aztec Diamond Tiling

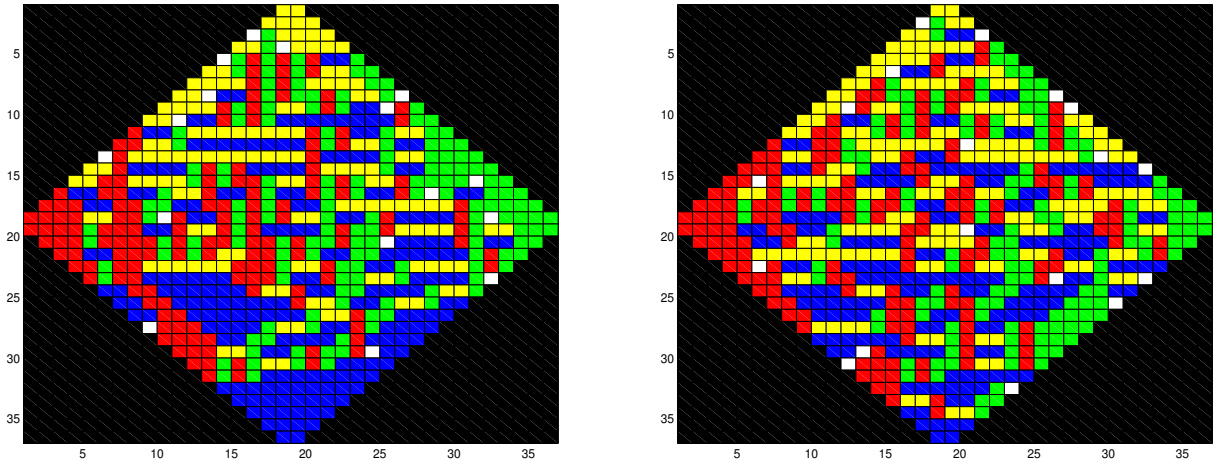

(Left) 16 Restricted (Right) 18 Restricted

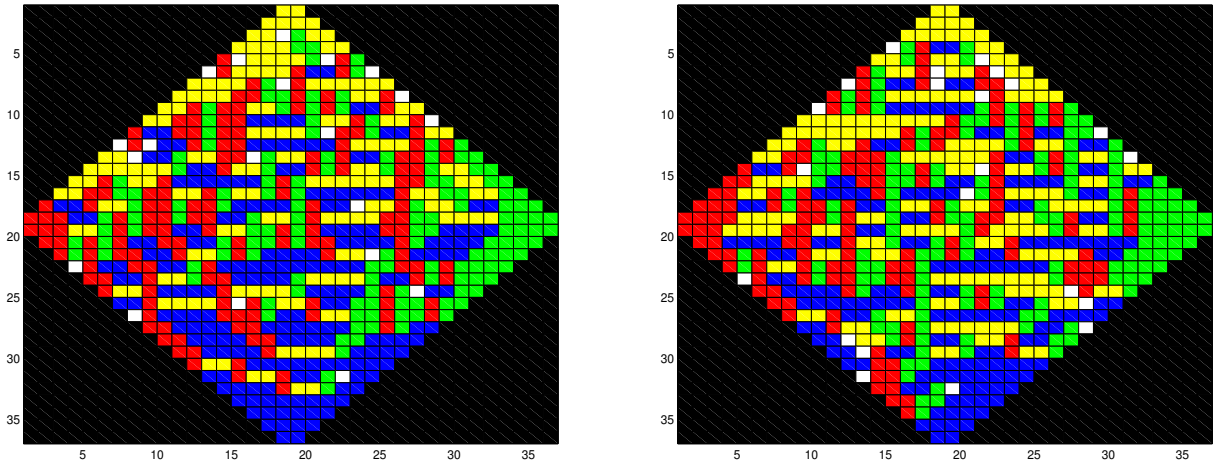

(Left) 20 Restricted (Right) 22 Restricted

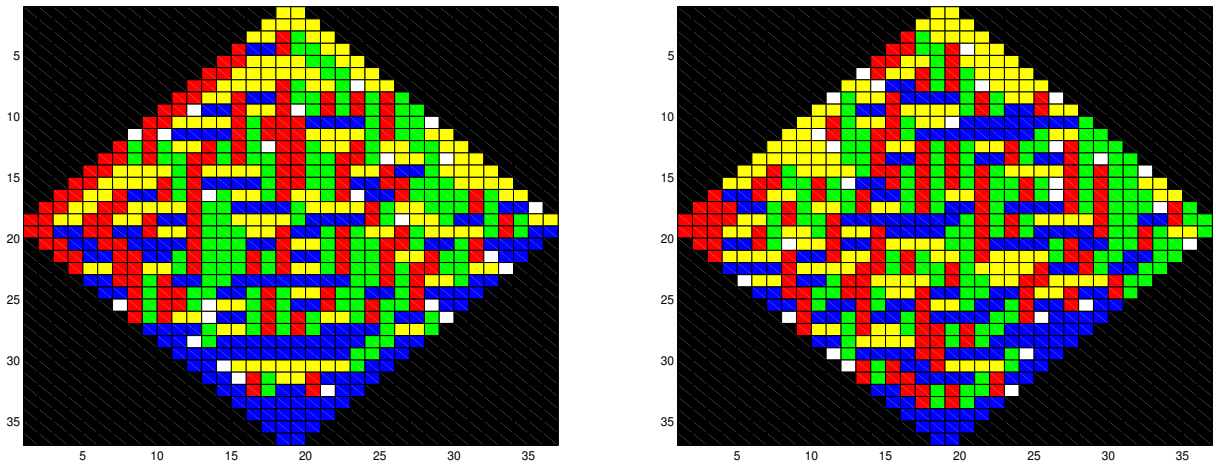

(Left) 24 Restricted (Right) 26 Restricted

Figure 3.9: We see a typical 16 Restricted Domino Aztec Diamond Tiling - a typical 26 Restricted Domino Aztec Diamond Tiling

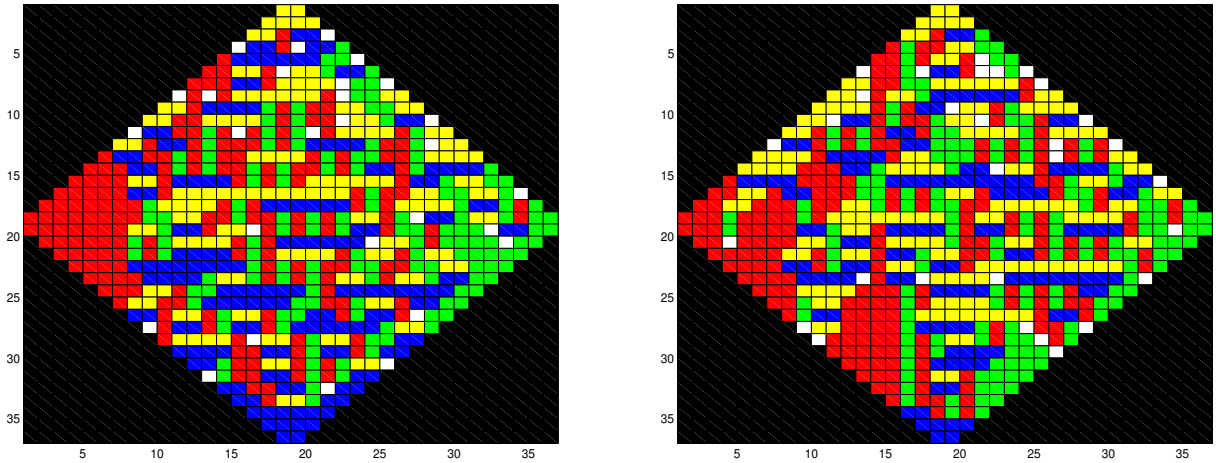

(Left) 28 Restricted (Right) 30 Restricted

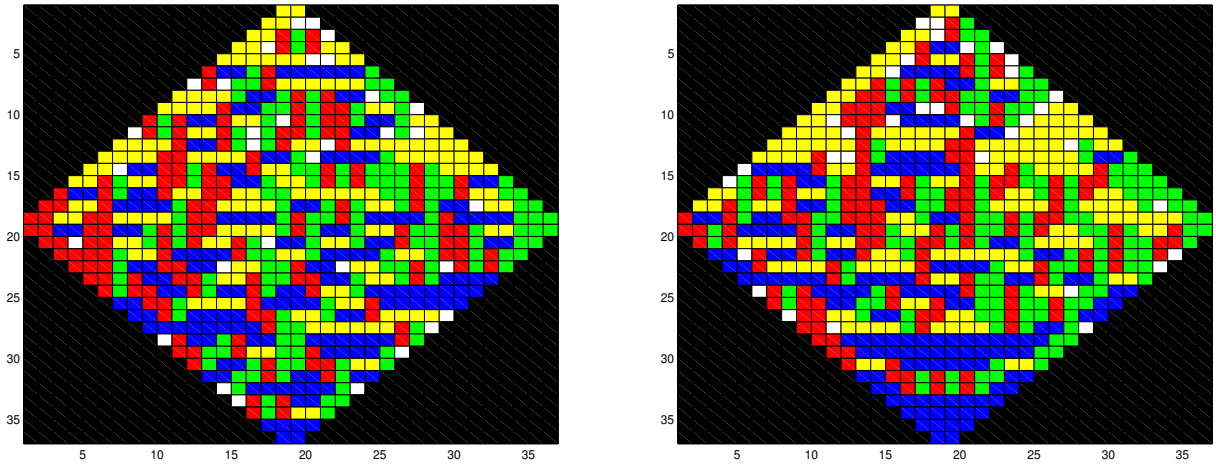

(Left) 32 Restricted (Right) 34 Restricted

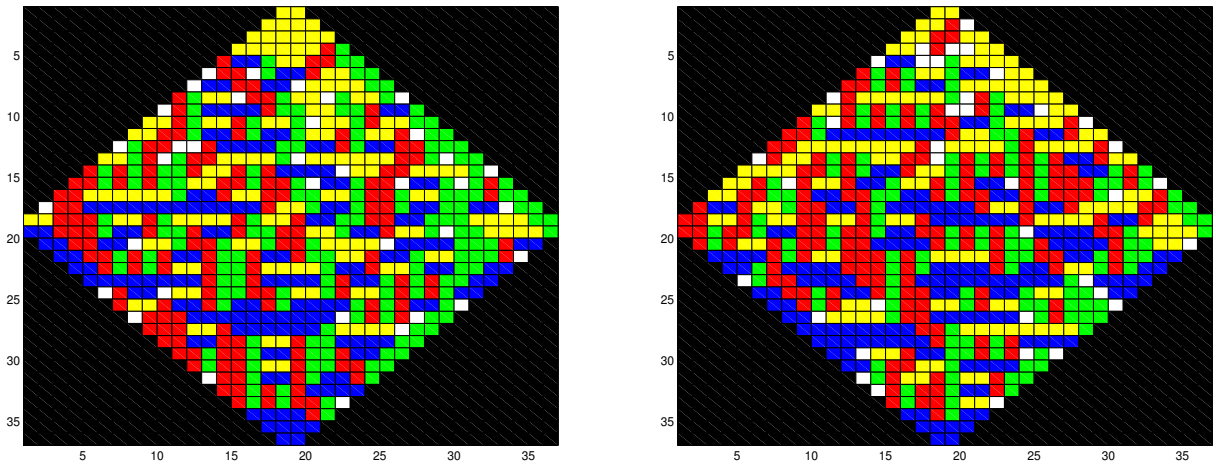

(Left) 36 Restricted (Right) 38 Restricted

Figure 3.10: We see a typical 28 Restricted Domino Aztec Diamond Tiling - a typical 38 Restricted Domino Aztec Diamond Tiling

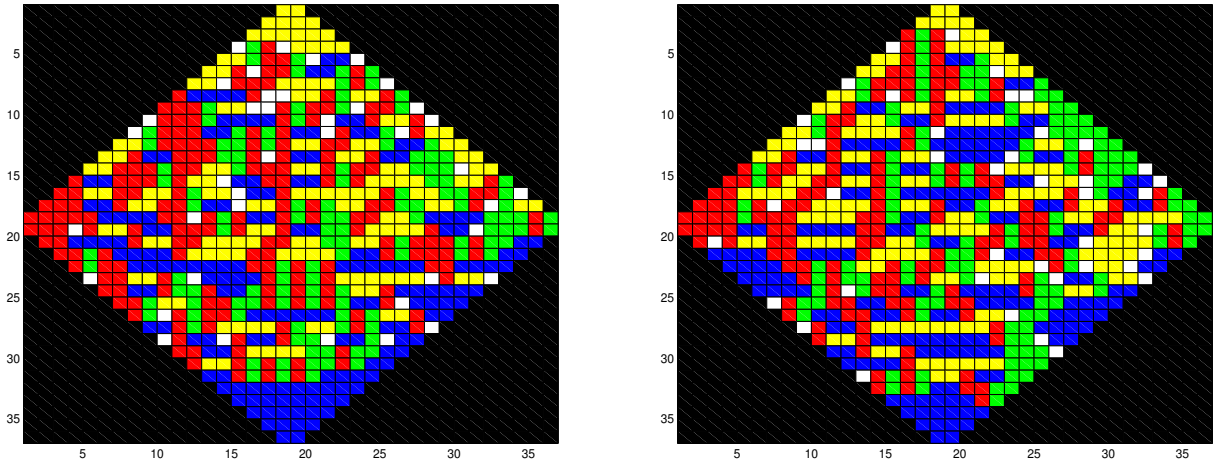

(Left) 40 Restricted (Right) 42 Restricted

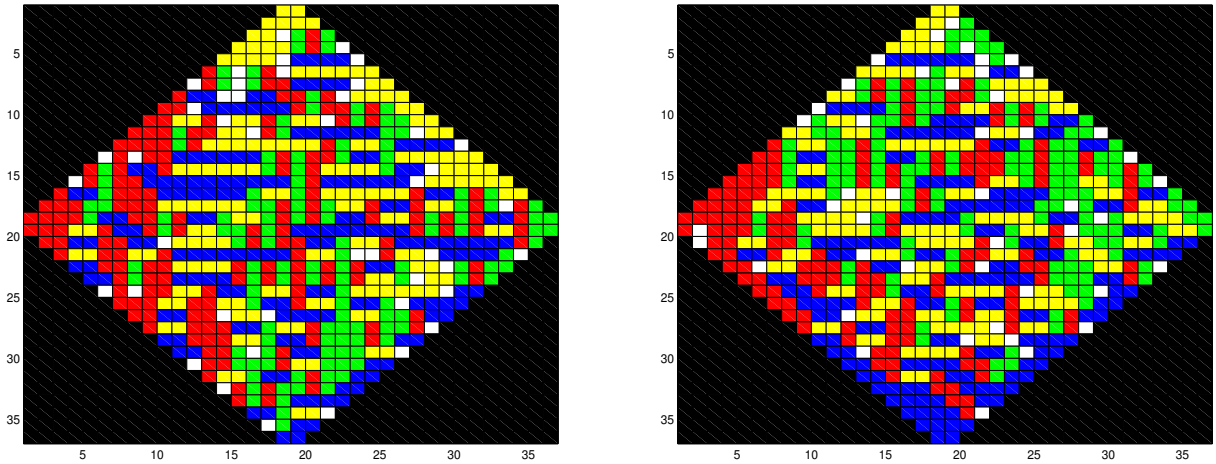

(Left) 44 Restricted (Right) 46 Restricted

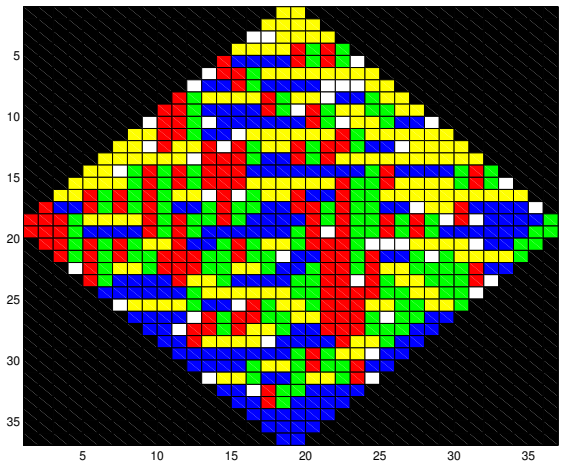

48 Restricted

Figure 3.11: We see a typical 40 Restricted Domino Aztec Diamond Tiling - a typical 48 Restricted Domino Aztec Diamond Tiling

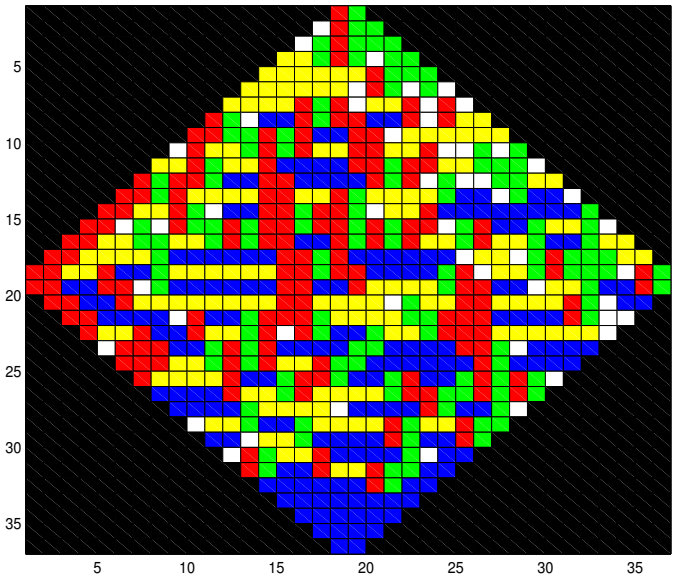

Figure 3.12: The Aztec Diamond with 50 voids after we apply the random walk five hundred million times.

3.5 Tight Packings

Next we wish to see if there is any structure in a tight domino packing on the Aztec Diamond. We notice in this case that our rules will be quite complicated. Not only do we want to be able to rotate the dominos and shift the empty spaces but also we want to be able to create and destroy empty spaces. And all three of these rules must be applied while maintaining the properties of a tight packing, in particular no two empty spaces may be adjacent. Each of our steps for this walk will include three rules:

1. The Rotation Rule
2. The Slide Rule
3. The Tetris Rule (Figure 3.13)

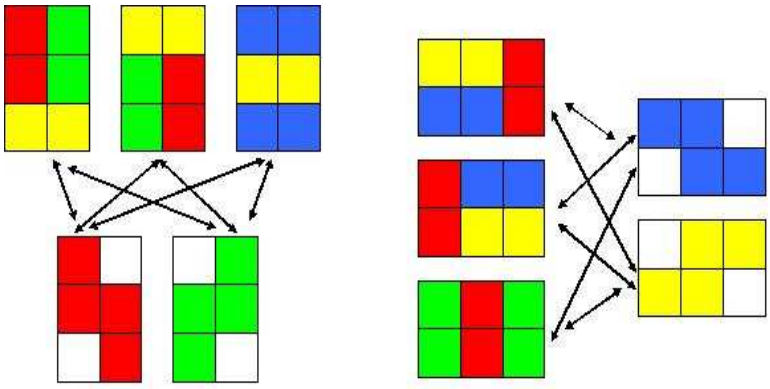

Figure 3.13: The tetris rule which we use during the steps in the tight Aztec Diamond packing.

The Rotation rule is the same as in the previous cases. The slide rule also remains the same but we must add a special check. Since we wish to maintain the *tightness* of the packing we must check to make sure our slide will uphold this property. Finally we apply the Tetris rule. We begin by at random choosing a 2×3 or 3×2 rectangle. We then check to see what is contained in the rectangle.

Case 1: We find two vertical adjacent dominos and one horizontal domino either on top or below the two vertical dominos or we find three adjacent horizontal dominos. We transform this into one of two vertical *tetris* rectangles. The first vertical tetris piece has empty squares in the top right and bottom left corners. The remainder of the rectangle contains two vertical dominos. The second vertical tetris rectangle has empty squares in the top left and bottom right corners. Once again the remainder of the rectangle is filled with two vertical dominos.

Case 2: We find our rectangle contains either of the vertical tetris rectangles. We transform into one of the three rectangles we mentioned in Case 1.

Case 3: We find two horizontal adjacent dominos and one vertical domino either on the left or on the right of the two vertical dominos or we find three adjacent vertical dominos. We transform this into one of two horizontal tetris rectangles. The first

horizontal tetris piece has empty squares in the top right and bottom left corners. The remainder of the rectangle contains two horizontal dominos. The second vertical tetris rectangle has empty squares in the top left and bottom right corners. Once again the remainder of the rectangle is filled with two horizontal dominos.

Case 4: We find our rectangle contains either of the horizontal tetris rectangles. We transform into one of the three rectangles we mentioned in Case 3.

Case 5: We are not in any of the previous cases we do nothing.

Once again we are interested in finding the typical tight Aztec Diamond packing. We do this by taking 500,000,000 steps on our random walk. We see in Figure 3.14 what a sample Aztec Diamond looks like.

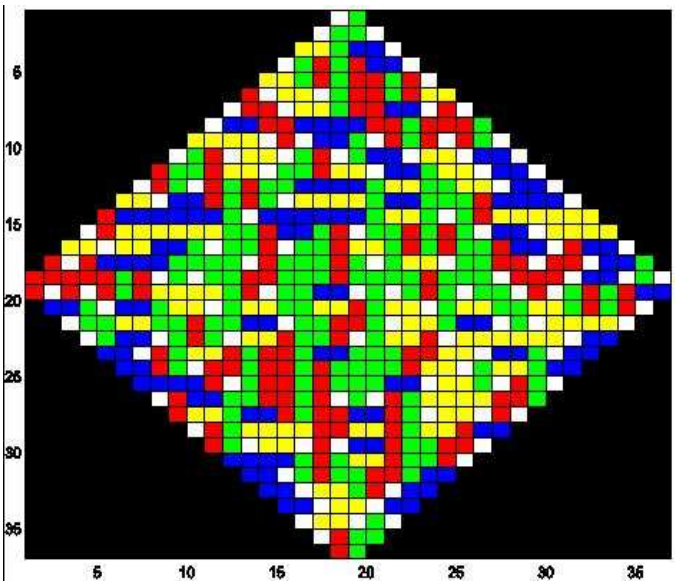

Figure 3.14: A tight Aztec Diamond after we apply the random walk five hundred million times.

3.6 Generalized Arctic Circle

There have been several attempts to find the Arctic Circle Phenomenon using new tilings on different spaces other then the Aztec Diamond. For example it has

been shown by [6] that a hexagon tiled with lozenges has a circular Arctic region [3].

Definition 3.6.1 Lozenge- A lozenge is a unit rhombus with angles $\frac{\pi}{3}$ and $\frac{2\pi}{3}$ [6].

Figure 3.15 shows the circular Arctic region discussed by [6, 3].

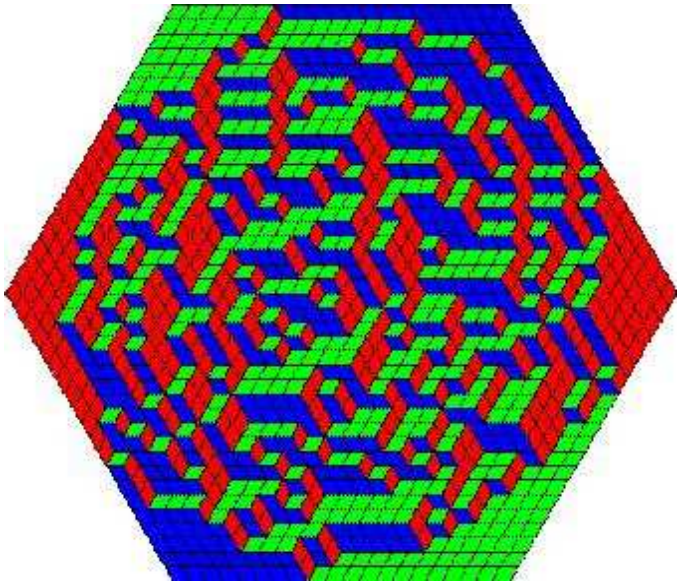

Figure 3.15: Another example of the Arctic Circle appearing in a hexagon tiled with lozenges.

3.6.1 4-omino Tilings on a Double Aztec Diamond

We are interested in exploring different tilings on a Double Aztec Diamond.

Definition 3.6.2 Double Aztec Diamond- A Double Aztec Diamond is an Aztec Diamond where the number of columns per each row are doubled as well as the number of rows per each column (Figure 3.16).

We wish to tile the Double Aztec Diamond with 1×4-ominos. We note that this case is not isomorphic to the domino tiling on the Aztec Diamond, since we are only doubling the domino lengthwise.

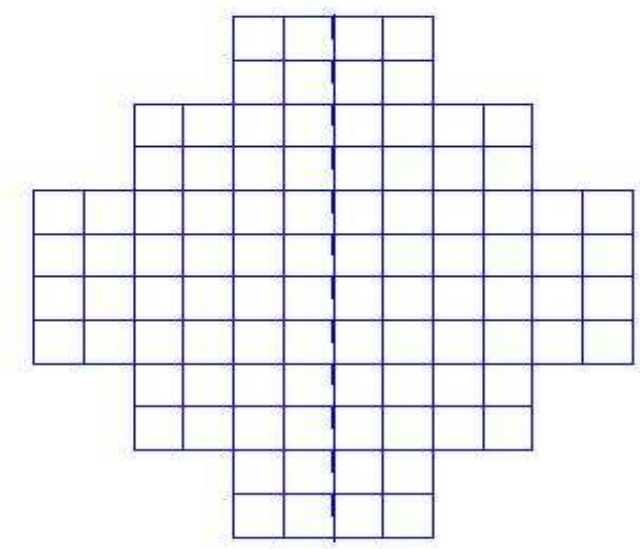

Figure 3.16: An order 4 Double Aztec Diamond.

Again we will use the Markov Chain Monte Carlo Method to find a typical tiling. We will use a Doubled Rotation Rule to complete our random walk. The Doubled Rotation Rule is as follows: Randomly choose a 4×4 area in the Aztec Diamond. We then check to see what is packing into this area.

Case 1: We find that there are four 4-ominos we simply rotate the 4-ominos. For example if we find four vertical 4-ominos we rotate these 4-ominos to create four horizontal 4-ominos (Figure 3.17).

Case 2: If there is an other combination of 4-ominos and pieces of 4-ominos we do nothing.

Each time we apply this rule, we consider the move a step. We apply 1,000,000,000 steps to find our typical tiling. Figure 3.18 shows an order 18 4-omino tiled Double Aztec Diamond and Figure 3.19 shows an order 30 4-omino tiled Double Aztec Diamond.

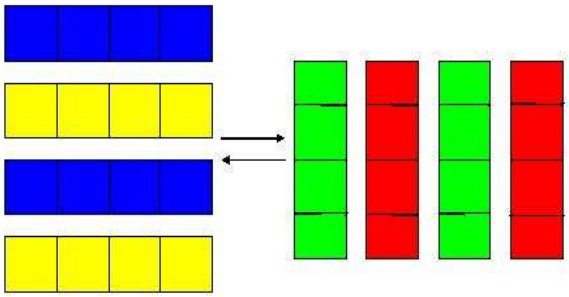

Figure 3.17: If we find four vertical 4-ominos we rotate them to four horizontal 4-ominos. Similarly if we find four horizontal 4-ominos we rotate to four vertical 4-ominos.

From Figure 3.18 and Figure 3.19 we see that when a 4-omino tiles a Double Aztec Diamond the typical packing appears to have a nice structure. We conjecture that as the order of our Double Aztec Diamond tends to ∞ the boundary of disordered tiles will form a a simple curve. It remains to continue researching this tiling to find the exact shape of this curve. Finally we wish to prove that our conjecture holds by following the procedure of using Ferries Graphs described by [22].

3.7 Concluding Remarks

We see that the domino tiling on the Aztec Diamond displays the Article Circle Phenomenon discussed by [22]. We also notice that both tight domino packings and non-tight domino packings on the Aztec Diamond have do not display the beautiful structure of the domino tiling. Finally we notice that if we created a restricted tiling with a certain number of voids the Article Circle Phenomenon slowly deteriorates and beings to lack structure similar to the tight and non-tight packings. Figure 3.20 shows a sample of all our different Aztec packings.

We are also interested in continuing to study our Doubled Aztec Diamonds. We wish to see if we can generalize the domino tiling theory to a $2n$-omino tiling

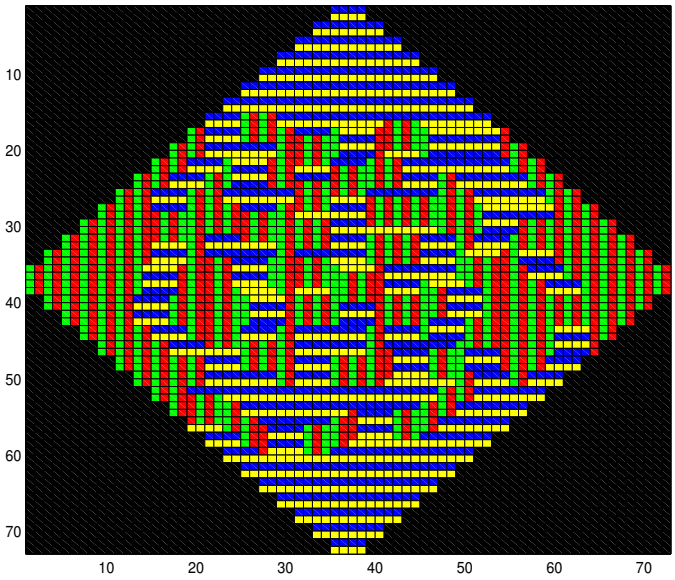

Figure 3.18: An order 18 Double Aztec Diamond tiled with 4-ominos.

theory on larger Aztec Diamonds. It also remains to show a proof that our 4-omino tiling on a Double Aztec Diamond displays a structure similar to the Arctic Circle Phenomenon.

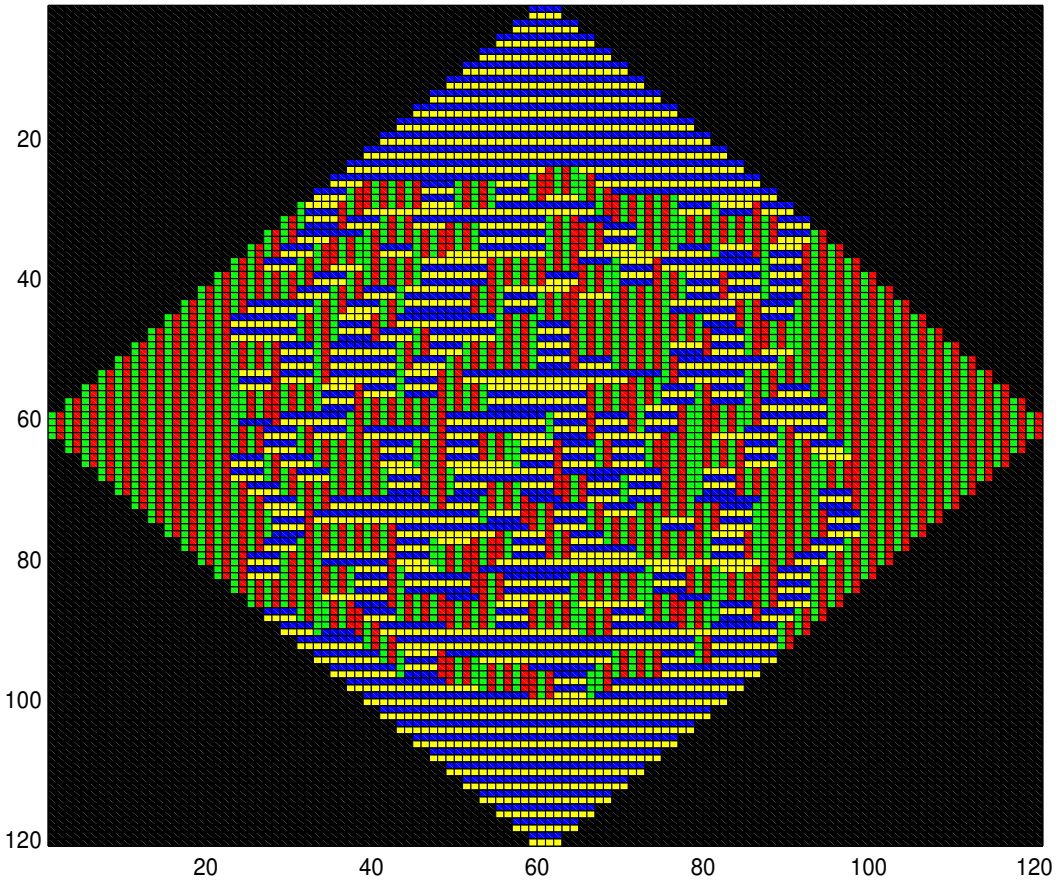

Figure 3.19: An order 30 Double Aztec Diamond tiled with 4-ominos.

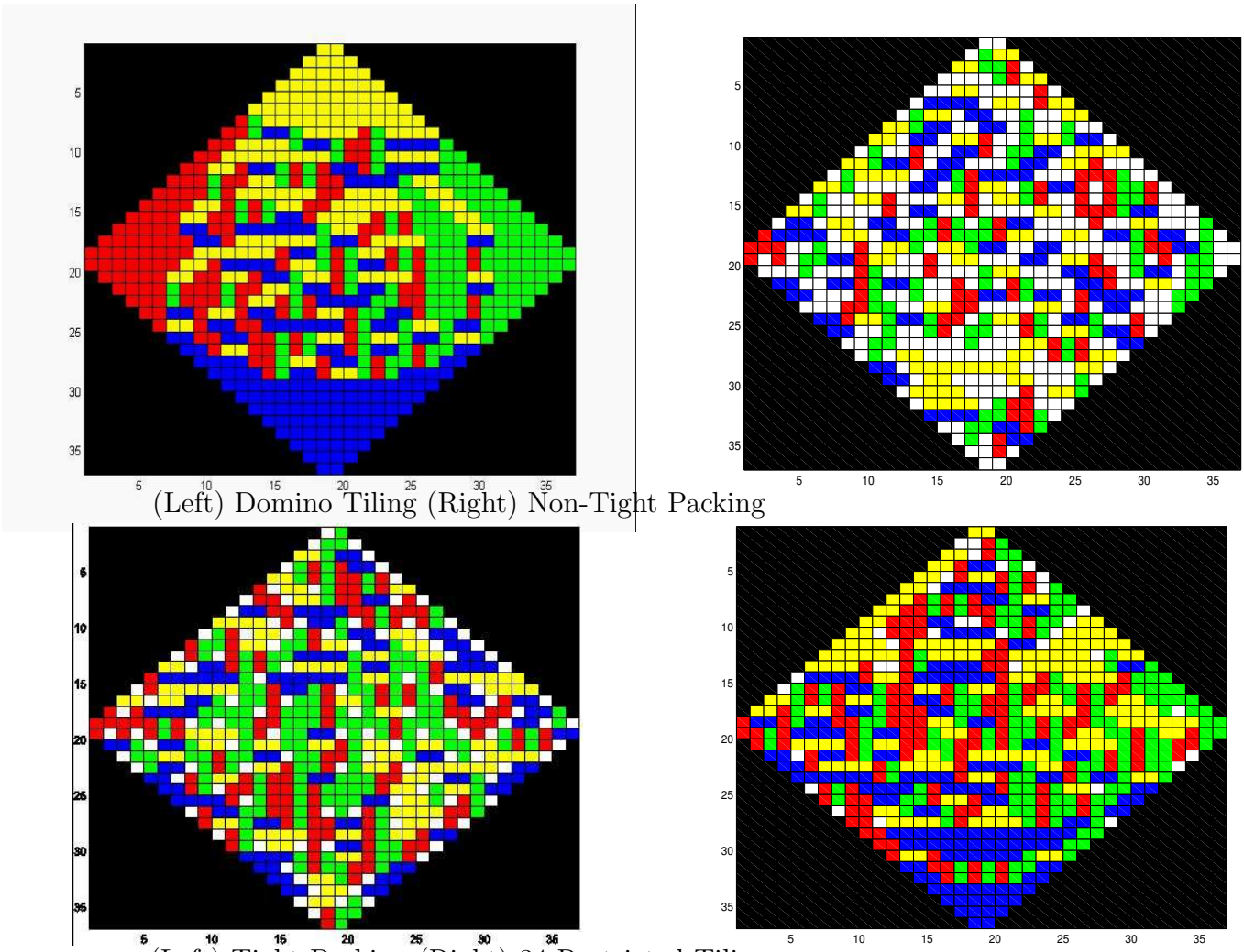

Figure 3.20: A sample of each different type of packing on the Aztec Diamond.

Appendix A

COMPUTER PROGRAMS

Listed below are descriptions of all computer programs used throughout our research. The pseudo codes of our Aztec Diamond simulations can be found in Appendix B.

- adjustMatrix(matrix)- Converts the given matrix so the dominos can be colored properly.
- aztecWalk4omTiling(order,start,lengthOfWalks,matrix)- Performs a random walk on a doubled Aztec Diamond tiled with 4-ominos for a specified number of times.
- aztecWalkDomTiling(order,start,lengthOfWalks,matrix)- Performs a random walk on a tiled Aztec Diamond for a specified number of times.
- aztecWalkNonTight(order,start,lengthOfWalks,matrix,tempVariable2)- Performs a random walk on a non-tight Aztec Diamond.
- aztecWalkTight(order,start,lengthOfWalks,matrix)- Performs a random walk on a tight Aztec Diamond.
- aztecWalkWithVoids(order,start,lengthOfWalks,matrix)- Performs a random walk on the given tiled Aztec Diamond with a certain number of voids.This function uses the function changeColor.

- changeColor(oldColor)- Function that will input the current color of some index in the Aztec Diamond. It will then change that color into the color of opposite parity. So for example when a blue horizontal domino is shifted left its color will change to a yellow horizontal domino.
- colorPacking(matrix)- Colors the current domino packing.
- colorPacking4omino(matrix)- Colors the current 4-omino packing
- create1DJominoPacking(j,n)- Creates a 1D non-tight jomino packing.
- create1DNonTightPacking(n)- Create a 1D non-tight domino packing.
- create1DTightPacking(n)- Creates a 1D tight domino packing.
- create2DNonTightPacking(n)- Creates an $n \times n$ non-tight domino packing.
- createAztec4omTiling(order)- Creates a 4-omino tiled doubled Aztec Diamond.
- createAztecDomTiling(order)- Creates a tiled Aztec Diamond with the specified order.
- createAztecDomTilingWithVoids(order,voids)- Creates an Aztec Diamond with the specified number of voids. Function uses createAztecDomTiling.
- createAztecNonTight(order)- Creates a non-tight aztec domino packing.
- exactMuNonTightDom(n)- Finds the void fraction for a non-tight 1D domino packing using the result from our analysis.
- nontight1DJominoWalk(j,n)- Performs a random walk on a 1D non-tight jomino packing and compute the average void fraction. Uses create1DJominoPacking.
- nonTight1DWalk(n)- Performs a random walk on a 1D non-tight packing and compute the average void fraction. Uses create1DNonTightPacking.

- nontight2DWalk(n,length,lengthEnd,matrix)- Performs a random walk on a 2D non-tight packing.

- nontightJomino(j,n)- will create a 1xn packing for a j-omino and perform a random walk to compute the average void fraction several times, to find the average void fraction.

- numberOf1DDomPackings(n)- Finds the total number of different packings for a domino on a $1 \times n$ chessboard.

- numberOf2DNonTightPackings(n)- Calculates the number of packings for a non-tight 2D packing.

- numPtsAsFunctionNonTight(j)- Plots the number of roots inside the unit circle, as a function of the jomino, for a non-tight 1D jomino. Uses numPtsInUnitNonTight.

- numPtsAsFunctionNonTightBucket(j)- Plots the number of roots inside the unit circle, as a function of the last jomino in the bucket, for a non-tight 1D bucket.Uses numPtsInUnitNonTightBucket.

- numPtsInUnit(j)- Calculates the number of roots that lie within the unit circle of a tight 1D jomino. Uses rootsofpoly.

- numptsinunitasfunction- Plots the number of roots that lie within the unit circle, for a tight jomino packing, as a function of the jomino.

- numPtsInUnitNonTight(j)- Calculates the number of roots that lie within the unit circle of a non-tight 1D jomino. Uses rootsOfNonTight.

- numPtsInUnitNonTightBucket(j)- Calculates the number of roots that lie within the unit circle of a non-tight 1D bucket packing. Uses rootsOfNonTightBucket.

- rootPlotNonTight(j)- Plots the roots of the singularities of the jomino. Uses rootsOfNonTight.
- rootPlotNonTight2- Plots multiple preset 1D non-tight jomino roots. Uses rootsOfNonTight.
- rootPlotNonTightBucket(j)- Plots the roots of the singularities of the non-tight 1D jomino bucket. Uses rootsOfNonTightBucket.
- rootsofjomino(j)- Finds the roots of a tight 1D jomino bucket packing.
- rootsOfNonTight(j)- Finds the roots of a non-tight 1D jomino packing.
- rootsOfNonTightBucket(j)- Finds the roots of a non-tight 1D jomino bucket packing.
- rootsofpoly(j)- Finds the roots of a tight 1D jomino packing.
- unitplot- Plots the unit circle.

Appendix B

AZTEC DIAMOND CODE

We will show the pseudo code for our Aztec Diamond simulations below.

B.1 Domino Tiling

First we create an Aztec Diamond using the createAztecDomTiling program.

Create a $2order \times 2order$ matrix.

Find the square that represents the first row, first column of our Aztec Diamond.

Randomly place either a vertical or horizontal domino.

Move to the next square in the Aztec Diamond. If we are at the end of the row move to the first column of the next row. If we are not at the end of the row, move to the next column in that row.

If it is empty, check to see if we can place an appropriate horizontal or vertical domino.

Repeat this process until we have tiled the diamond.

Next we shall apply the random walk using the aztecWalkDomTiling program.

Choose a random square in the Aztec Diamond.

Randomly choose a 2x2 square that contains that square.

Apply the Rotation Rule(Figure B.1)

Check to see what is contained in the square.

If we find two horizontal dominos change the square to two vertical dominos.

If we find two vertical dominos change it to two horizontal dominos.

If we are not in either of these cases do nothing.

Repeat this process until we have completed the correct number of steps.

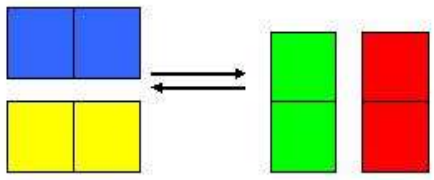

Figure B.1: If we find two vertical dominos we replace them with two horizontal dominos and vise versa.

B.2 Non-Tight Aztec Packing

First we create an Aztec Diamond using the createAztecNonTight program

Create a $2order \times 2order$ matrix.

Find the square which will be the first row, first column of our Aztec Diamond.

Randomly place either a vertical domino, a horizontal domino, or an empty space.

Move to the next square in the Aztec Diamond. If we are at the end of the row move to the first column of the next row. If we are not at the end of the row, move to the next column in that row.

If the next square is empty, check to see if we can place an appropriate vertical domino, horizontal domino or empty space.

Repeat this process until the Aztec Diamond is non-tightly packed.

Next we shall apply the random walk using the aztecWalkNonTight program.

Randomly choose one square in the Aztec Diamond.

Randomly choose either a 1×2 or 2×1 rectangle that contains that square.

Check to see what is in that rectangle.

If there is a domino, remove it.

If there are two empty spaces add a domino.

If there is an other combination of domino parts and empty spaces, do nothing.

Repeat the process until we have completed the correct number of steps.

B.3 Restricted Aztec Diamond Tilings

First we create an Aztec Diamond using the createAztecDomTilingWithVoids program

Create a domino tiled Aztec Diamond using createAztecDomTiling.

Choose a random square in the Aztec Diamond.

If the square is empty do nothing.

If the square is not empty, remove the domino that we find there.

Continue this process until we have the specified number of empty spaces.

Next we shall apply the random walk using the aztecWalkWithVoids program.

Randomly choose a square in the Aztec Diamond.

Randomly choose a 2x2 square that contains that square.

Apply the Rotation Rule (Figure B.1):

Check to see what is contained in the square.

If we find two horizontal dominos change the square to two vertical dominos.

If we find two vertical dominos change it to two horizontal dominos.

If we are not in either of these cases do nothing.

Next apply the Slide Rule (Figure B.2):

Randomly choose one square in the Aztec Diamond.

At random slide a vertical or horizontal domino into the current empty square and move the empty square to the far end of the domino.

Repeat this process until we have completed the correct number of steps.

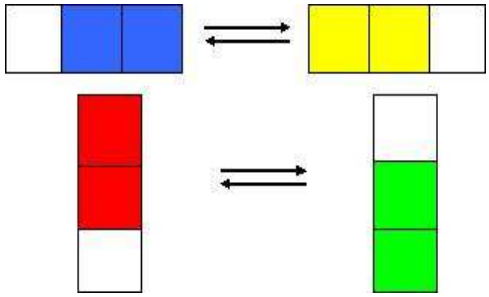

Figure B.2: The aztec diamond tiled with dominos.

B.4 Tight Aztec Diamond Packings

First we create an Aztec Diamond using the createAztecDomTiling

Next we shall apply the random walk using the aztecWalkTight program.

Randomly choose a square in the Aztec Diamond.

Randomly choose a 2x2 square that contains that square.

Apply the Rotation Rule (Figure B.1):

Check to see what is contained in the square.

If we find two horizontal dominos change the square to two vertical dominos.

If we find two vertical dominos change it to two horizontal dominos.

If we are not in either of these cases do nothing.

Next apply the Slide Rule (Figure B.2):

Randomly choose one square in the Aztec Diamond.

At random slide a vertical or horizontal domino into the current empty square and move the empty square to the far end of the domino. (Careful that the slide will uphold the tightness of the packing.)

Finally we apply the Tetris Rule(Figure B.3):

Choose one square at random.

Choose a 2×3 or 3×2 rectangle within the Aztec Diamond that contains that

square.

Check to see what is contained in the rectangle.

If we find two vertical adjacent dominos and one horizontal domino either on top or below the two vertical dominos or we find three adjacent horizontal dominos. We transform this into one of two vertical *tetris* rectangles. The first vertical tetris piece has empty squares in the top right and bottom left corners. The remainder of the rectangle contains two vertical dominos. The second vertical tetris rectangle has empty squares in the top left and bottom right corners. Once again the remainder of the rectangle is filled with two vertical dominos.

If we find our rectangle contains either of the vertical tetris rectangles. We transform into one of the three rectangles we mentioned in above.

If we find two horizontal adjacent dominos and one vertical domino either on the left or on the right of the two vertical dominos or we find three adjacent vertical dominos. We transform this into one of two horizontal tetris rectangles. The first horizontal tetris piece has empty squares in the top right and bottom left corners. The remainder of the rectangle contains two horizontal dominos. The second vertical tetris rectangle has empty squares in the top left and bottom right corners. Once again the remainder of the rectangle is filled with two horizontal dominos.

If we find our rectangle contains either of the horizontal tetris rectangles. We transform into one of the three rectangles we mentioned above.

If we are not in any of the previous cases we do nothing.

We repeat these three rules until we have completed the correct number of steps.

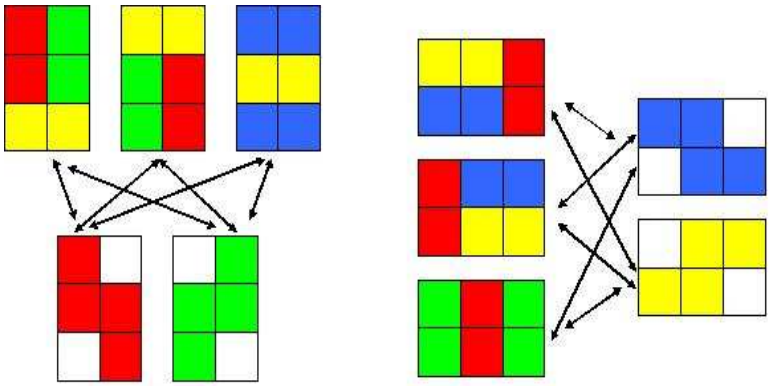

Figure B.3: The tetris rule which we use during the steps in the tight aztec diamond packing.

BIBLIOGRAPHY

[1] A.F. Archer. A modern treatment of the 15-puzzle. *The Amer. Math. Monthly*, 106(9):793–799, 1999.

[2] Tomaso Aste and Denis Weaire. *The Pursuit of Perfect Packing*. Institute of Physics Publilshing, Philadelphia, PA, USA, 2000.

[3] Matthew Blum. Arctic behavior in random tilings. 1997.

[4] B.J. Buchalter and R.M. Bradley. Orientational order in amorphous packings of ellipses. *J. Phys. A: Math. Gen.*, 25:L1219–L1224, 1992.

[5] S. Chib and E. Greenberg. Understanding the metropolis-hastings algorithm. *The Amer. Stat.*, 49(4):327–335, 1995.

[6] Henry Cohn, Michael Larsen, and James Propp. The shape of a typical boxed plane partition. *New York J. Math*, pages 137 – 165, 1996.

[7] A. Donev, I. Cisse, D. Sachs, E.A. Variano, F. H. Stillinger, R. COnnelly, S. Torquato, and P.M. Chaikin. Optimal particle packings: Problems for the ages. *Science*, 303:990–993, 2004.

[8] G. Fiumara and P.V. Giaquinta. Equilibrium versus random sequential addition of dimers on a lattice. *J. Phys. A: Math. Gen.*, 27:4351–4358, 1994.

[9] S. Franklin. *piggy.rit.edu/franklin*, 2003.

[10] Solomon W. Golomb. *Polyominoes*. Princeton University Press, Princeton, NJ, USA, 1994.

[11] M. Grumann, M. Dobmeier, P. Schippers, T. Brenner, R. Zengerle, and J. Ducree. The model of porous media - complete description of the aggregation of bead-monolayers in flat microfluidic chambers. *Proc. of Nanotech 2004*, 2:383–386, 2004.

[12] M. Grumann, P. Schippers, M. Dobmeier, S. Haberle, A. Geipel, T. Brenner, R. Zengerle, and J. Ducree. Formation of hexagonal monolayers by flow of bead suspensions into flat micro-chambers. *Proc. of IMECE 2003*, pages 1–5, 2003.

[13] E.L. Hinrichsen, J. Feder, and T. Jossang. Random packing of disks in two dimensions. *Phys. Rev. A*, 41:4199–4209, 1990.

[14] E.H. Kuo. *MIT Undergraduate Jrnl. of Math.*, 1:111–121, 1998.

[15] B. Littlewood and J.L. Verrall. Random sequential addition of hard atoms to the one-dimensional integer lattice. *Jrnl. Chem. Phys.*, 59:1613–1615, 1973.

[16] M. Luby, D. Randall, and A. Sinclair. Markov chain algorithms for planar lattice structures. *SIAM Jrnl. on Computing*, 31:167–192, 2001.

[17] J. A. Morrison. The minimum of gaps generated by random packing of unit intervals into a large interval. *SIAM J. Appl. Math*, 47:398–410, 1987.

[18] M.A. Novotny. Introduction to the propp-wilson method of exact sampling for the ising model. *Computer Simulation Studies in Condensed Matter Physics XII*, pages 179–184, 2000.

[19] J.J. O'Connor and E.F. Robertson. The mactutor history of mathematics archive, 2006. http://www-history.mcs.stAndrews.ac.uk/history/index.html.

[20] Department of Math and Dickinson College Computer Science. Puzzles of the month, 2006. http://www.dickinson.edu/departments/mathcs/puzzle/oldindex.html.

[21] C.J. Olson, C. Reichhardt, M. McCloskey, and R.J. Zieve. Effect of grain anisotropy on ordering, stability and dynamics in granular systems. *Europhys. Lett.*, 6:904–910, 2002.

[22] J.G. Propp and D.B. Wilson. Exact sampling with coupled markov chains and applications to statistical mechanics. *Random Structures and Algorithms*, 9:223–252, 1996.

[23] I.C. Rankenburg and R.J. Zieve. The influence of shape on ordering of granular systems in two dimensions. *Phys. Rev. E*, 63, 2001.

[24] A. Rényi. On a one-dimensional problem concerning random space-filling. *Publ. Math. Inst. Hung. Acad. Sci.*, 3:109–127, 1958.

[25] J.D. Sherwood. Packing of spheroids in three-dimensional space by random sequential addition. *J. Phys. A: Math. Gen.*, 30:L839–L843, 1997.

[26] P.F. Stadler, J.M. Luck, and A. Mehta. Ratchet-induced segregation of non-spherical grains. *Europhys. Lett.*, 57:46–52, 2001.

[27] K. Stokely, A. Diacou, and S.V. Franklin. Two-dimensional packing in prolate granular materials. *Phys. Rev. E*, 67, 2003.

[28] James Tanton. A dozen questions about fibonacci numbers. *Math Horizons*, pages 5 – 9, 2005.

[29] T.Okubo and T. Odagaki. Random packing of binary hard discs. *Jrnl. of Phys. Condensed Matter*, 16:6651–6659, 2004.

[30] A.M. Verhagen. Exclusion problem for mobile atoms of any size in one dimension. *Jrnl. Chem. Phys.*, 53:2226–2230, 1970.

[31] F.X. Villarruel, B.E. Lauderdale, D.M. Mueth, and H.M. Jaeger. Compaction of rods: Relaxation and ordering in vibrated, anisotropic granular material. *Phys. Rev. E*, 61:6914–6921, 2000.

[32] D. Won and C. Kim. Alignment and aggregation of spherical particles in viscoelastic fluid under shear flow. *J. Non-Newtonian Fluid Mech.*, 117:141–146, 2004.